

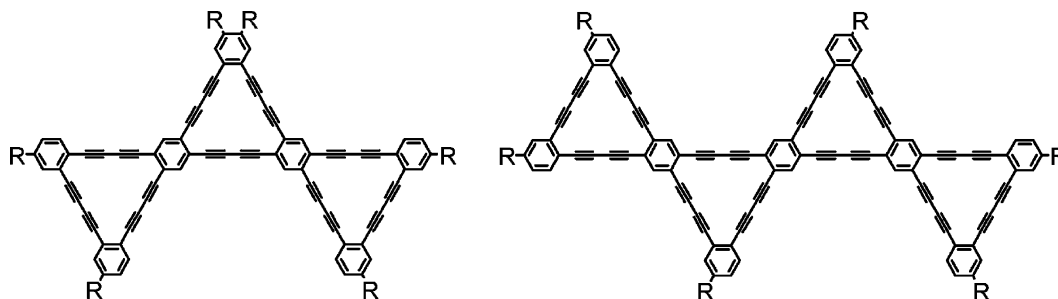
Carbon Networks Based on Dehydrobenzoannulenes. 5. Extension of Two-Dimensional Conjugation in Graphdiyne Nanoarchitectures

Jeremiah A. Marsden and Michael M. Haley*

Department of Chemistry, Materials Science Institute, and Oregon Nanosciences and Microtechnologies Institute, University of Oregon, Eugene, Oregon 97403-1253

haley@uoregon.edu

Received May 9, 2005

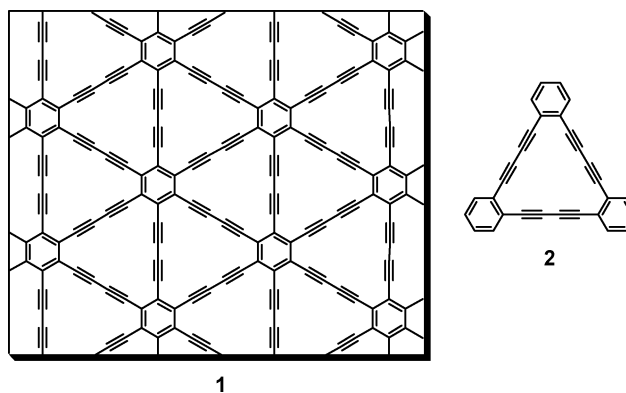


The synthesis and optical properties of a series of multinanometer-sized substructures of the phenyl-diacetylene carbon allotrope, graphdiyne, are described. These molecules are among the largest and most complex annulenic systems yet prepared, with extension of linear conjugation in two-dimensions to over twice that of any previously reported planar macrocycle. The graphdiyne substructures are constructed through convergent syntheses, taking advantage of three key intermediates and silane-protected phenylacetylenes. Intramolecular macrocyclization of α,ω -polykyne precursors via Cu-mediated or Pd-catalyzed oxidative homocoupling affords five new graphdiyne “oligomers” possessing two to four fused 18-membered rings. The attempted synthesis of a six-ring analogue is also reported.

Introduction

Over the past 20 years, highly conjugated organic materials have been recognized as ideal candidates for use in next-generation electronic and optoelectronic devices and media because of their unique electrical, optical, and structural properties.¹ Organic materials are of particular attraction due to the ease of structural fine-tuning to enhance specific properties for specialized applications such as optical switches, thin-film transistors, liquid crystals, optical storage devices, etc.² Phenylacetylenes are a key class of highly conjugated organic materials that have seen extensive study for use in such advanced applications owing in large part to their highly polarizable π -electrons and structural rigidity.³

As part of our ongoing studies of phenylacetylene systems,⁴ we have focused much of our efforts on the



preparation of increasingly larger substructures of the theoretical all-carbon network graphdiyne (1).⁵ Graph-

diyne is predicted to exhibit fascinating properties including high third-order nonlinear optical (NLO) susceptibility, high fluorescence efficiency, extreme hardness, thermal resistance, conductivity or superconductivity, and through-sheet transport of ions.^{5,6} With a calculated heat of formation of 18.3 kcal per gram-atom and virtually no strain energy,⁷ it is predicted to be the most stable carbon allotrope containing diacetylene linkages and therefore one of the most “synthetically approachable”.^{5a,8} Direct preparation of graphdiyne, however, has not yet been successful,⁹ therefore, as previously reported,^{7,10} we have constructed model substructures based on its simplest macrocyclic unit, dodecadehydrotribenzo[18]annulene (DBA, **2**). Intrigued by early failed attempts at **2** and other similar annulenic systems via intermolecular cyclooligomerization,¹¹ which resulted mainly in inseparable mixtures of dimer, trimer, and tetramer,^{4,9b,11d,12} we

utilized an intramolecular cyclization procedure by means of α,ω -polyynes under pseudo high-dilution homocoupling conditions. Using this methodology, we successfully constructed **2** and several additional two- and three-ring fused graphdiyne substructures.^{4,7,10}

We have been particularly interested in the electronic absorption properties of the graphdiyne subunits, which provide clues to the potential for further optical properties such as NLO susceptibility and two-photon absorption.¹³ The remarkable optical properties of graphdiyne “oligomers” presumably arise from the extended two-dimensional π -conjugation present in the systems. The extent of delocalization is apparent by bathochromic shifts in the UV–vis absorption spectra. We found that the largest bathochromic shifts displayed by graphdiyne substructures belonged to the systems possessing the longer linear *p*-bis(phenylbutadiynyl)benzene chromophores, indicating that enhanced optical effects are more a function of effective linear conjugation length than macrocycle size or molecular weight.^{7b} We have therefore designed larger graphdiyne substructures possessing further extension of linear conjugation in two dimensions with hopes to increase the effective π -delocalization and to provide further clues to the bulk properties of the theoretical all-carbon network. The syntheses of macrocycles **3–6** and attempts at **7** are herein reported, as well as a discussion of their optical absorption and emission characteristics.

Results and Discussion

Retrosynthesis. The common feature present in all previously reported bis- and tris[18]annulenes was a central symmetrical benzene ring onto which each macrocycle was fused. To prepare larger systems with fusion in patterns other than to a central ring, the previous methodology needed modification. To address this, asymmetric coupling piece **8**, composed of one and a half precyclized 18-membered rings, was designed (Scheme 1). The butadiynyl terminus of this component can be cross-coupled to a variety of haloarene units followed by multiple intramolecular cyclizations to give the “super-sized” graphdiyne substructures **3–7**. To control placement of each alkyne unit during the construction of “key piece” **8**, the 1,2,4,5-substituted asymmetric arene **9** possessing three different coupling positions was designed and synthesized in four steps from a known precursor.

Another important issue that needed addressing for the successful construction of larger annulenic structures was the poor solubility of the planar DBAs. During the syntheses of prior graphdiyne subunits, solubility became a problem with substructures possessing more than one 18-membered ring; therefore, solubilizing appendages such as *tert*-butyl and *n*-decyl were built into the systems

(1) Inter alia: (a) Chen, J.; Reed, M. A.; Dirk, S. M.; Price, D. W.; Rawlett, A. M.; Tour, J. M.; Grubisha, D. S.; Bennett, D. W. In *NATO Science Series, II: Mathematics, Physics, Chemistry (Molecular Electronics: Bio-Sensors and Bio-Computers)*; Plenum: New York, 2003; Vol. 96, pp 59–195. (b) Domerco, B.; Hreha, R. D.; Zhang, Y.-D.; Haldi, A.; Barlow, S.; Marder, S. R.; Kippelen, B. *J. Polym. Sci., Part B: Polym. Phys.* **2003**, *41*, 2726–2732. (c) Shirota, Y. *J. Mater. Chem.* **2000**, *10*, 1–25. (d) Schwab, P. F. H.; Levin, M. D.; Michl, J. *Chem. Rev.* **1999**, *99*, 1863–1933. (e) *Electronic Materials: The Oligomer Approach*; Müllen, K., Wegner, G., Eds.; Wiley-VCH: Weinheim, Germany, 1998. (f) Tour, J. M. *Chem. Rev.* **1996**, *96*, 537–562. (g) *Photonic and Optoelectronic Polymers*; Jenekhe, S. A., Wynne, K. J., Eds.; American Chemical Society: Washington, DC, 1995. (h) Special Issue: *Chem. Rev.* **1994**, *94*, 1–278. (i) *Conjugated Polymers and Related Materials. The Interconnection of Chemical and Electronic Structure*; Lunström, W. R., Salaneck, I., Rånby, B., Eds.; Oxford Press: Oxford, 1993.

(2) Recent examples, inter alia: (a) Seminario, J. M. *Nat. Mater.* **2005**, *4*, 111–113. (b) Hughes, G.; Bryce, M. R. *J. Mater. Chem.* **2005**, *15*, 94–107. (c) Van der Auweraer, M.; De Schryver, F. C. *Nat. Mater.* **2004**, *3*, 507–508. (d) Special Issue on Organic Electronics: *Chem. Mater.* **2004**, *16*, 4381–4846. (e) Wong, M. S.; Li, Z. H.; Tao, Y.; D'Iorio, M. *Chem. Mater.* **2003**, *15*, 1198–1203. (f) Cornil, J.; Beljonne, D.; Calbert, J.-P.; Brédas, J.-L. *Adv. Mater.* **2001**, *13*, 1053–1067.

(3) Inter alia: (a) Zhao, Y.; Slepokov, A. D.; Akoto, C. O.; McDonald, R.; Hegmann, F. A.; Tykwinski, R. R. *Chem. Eur. J.* **2005**, *11*, 321–329. (b) Fasina, T. M.; Collings, J. C.; Lydon, D. P.; Albesa-Jove, D.; Batsanov, A. S.; Howard, J. A. K.; Nguyen, P.; Bruce, M.; Scott, A. J.; Clegg, W.; Watt, S. W.; Viney, C.; Marder, T. B. *J. Mater. Chem.* **2004**, *14*, 2395–2404. (c) Gonzalo-Rodriguez, J.; Esquivias, J.; Lafuente, A.; Diaz, C. *J. Org. Chem.* **2003**, *68*, 8120–8128. (d) Nielsen, M. B.; Diederich, F. In *Modern Arene Chemistry*; Astruc, D., Ed.; Wiley-VCH: Weinheim, Germany, 2002; pp 196–216. (e) Bunz, U. H. F. *Chem. Rev.* **2000**, *100*, 1605–1644.

(4) (a) Marsden, J. A.; Palmer, G. J.; Haley, M. M. *Eur. J. Org. Chem.* **2003**, 2355–2369. (b) Jones, C. S.; O'Connor, M. J.; Haley, M. M. In *Acetylene Chemistry—Chemistry, Biology, and Material Science*; Diederich, F., Stang, P. J., Tykwinski, R. R., Eds.; Wiley-VCH: Weinheim, Germany, 2005; pp 303–385.

(5) (a) Haley, M. M.; Wan, W. B. In *Advances in Strained and Interesting Organic Molecules*; Halton, B., Ed.; JAI Press: Greenwich, 2000; Vol. 8, pp 1–41. (b) Baughman, R. H.; Eckhardt, H.; Kertesz, M. *J. Chem. Phys.* **1987**, *87*, 6687–6699.

(6) (a) Balaban, A. T.; Rentia, C. C.; Ciupitu, E. *Rev. Roum. Chim.* **1968**, *13*, 231–247. (b) Narita, N.; Nagai, S.; Suzuki, S.; Nakao, K. *Phys. Rev. B* **1998**, *58*, 11009–11014. (c) Narita, N.; Nagai, S.; Suzuki, S.; Nakao, K. *Phys. Rev. B* **2000**, *62*, 11146–11151. (d) Narita, N.; Nagai, S.; Suzuki, S. *Phys. Rev. B* **2001**, *64*, 245–248. (e) Kondo, M.; Nozaki, D.; Tachibana, M.; Yumura, T.; Yoshizawa, K. *Chem. Phys.* **2005**, *312*, 289–297.

(7) (a) Haley, M. M.; Brand, S. C.; Pak, J. *J. Angew. Chem., Int. Ed. Engl.* **1997**, *36*, 836–838. (b) Wan, W. B.; Brand, S. C.; Pak, J. J.; Haley, M. M. *Chem. Eur. J.* **2000**, *6*, 2044–2052.

(8) (a) Rubin, Y.; Diederich, F. *Angew. Chem., Int. Ed. Engl.* **1992**, *31*, 1101–1164. (b) Diederich, F. *Nature (London)* **1994**, *369*, 199–207. (c) Bunz, U. H. F.; Rubin, Y.; Tobe, Y. *Chem. Soc. Rev.* **1999**, 107–119.

(9) (a) Dierks, R.; Armstrong, J. C.; Boese, R.; Vollhardt, K. P. C. *Angew. Chem., Int. Ed. Engl.* **1986**, *36*, 268–269. (b) Tovar, J. D.; Jux, N.; Jarrosson, T.; Khan, S. I.; Rubin, Y. *J. Org. Chem.* **1997**, *62*, 3432–3433.

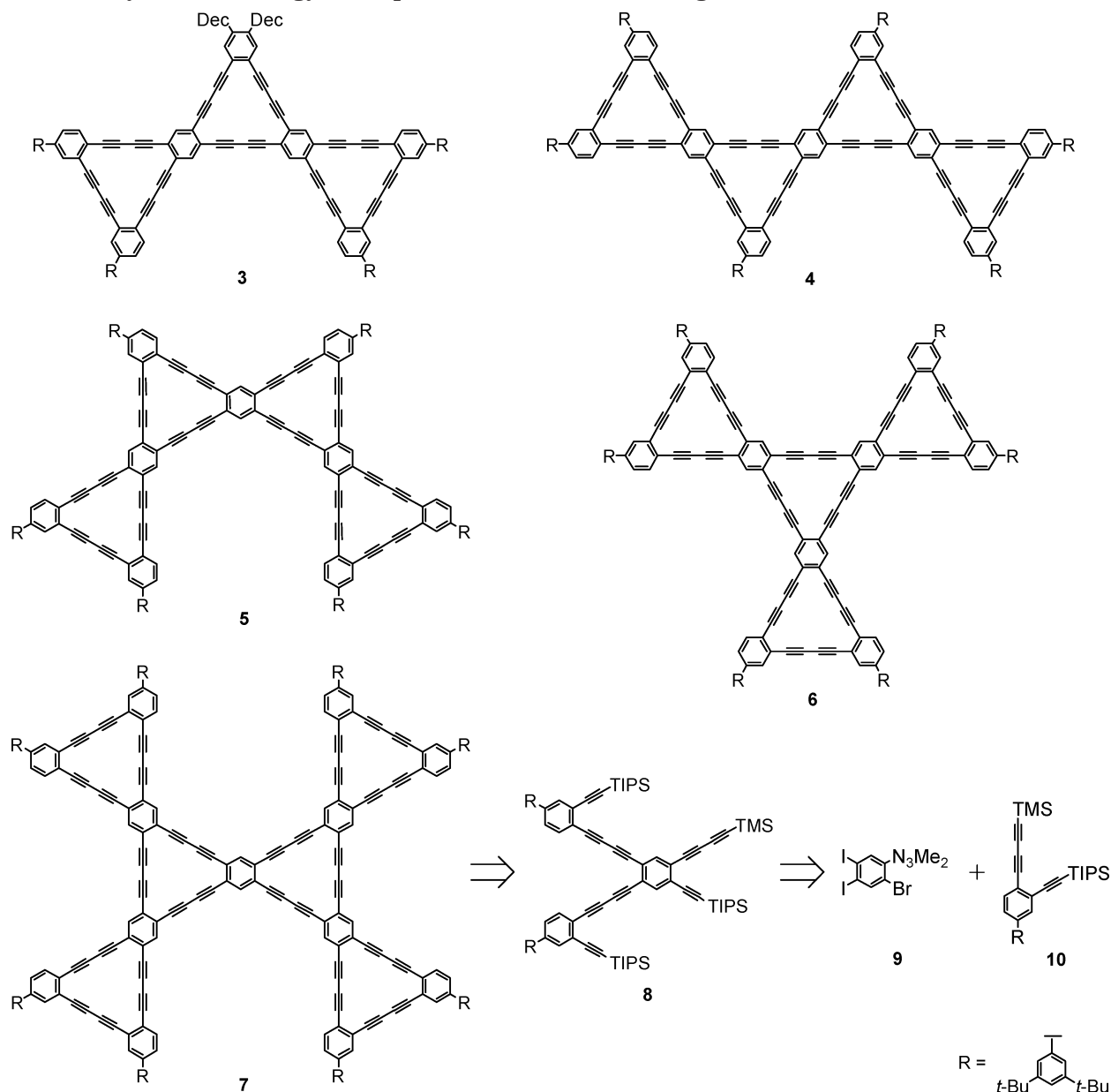
(10) Wan, W. B.; Haley, M. M. *J. Org. Chem.* **2001**, *66*, 3893–3901.

(11) (a) Eglinton, G.; Galbraith, A. R. *Proc. Chem. Soc.* **1957**, 350–351. (b) Behr, O. M.; Eglinton, G.; Raphael, A. R. *Chem. Ind.* **1959**, 699–700. (c) Eglinton, G.; Galbraith, A. R. *J. Chem. Soc.* **1960**, 3614–3625. (d) Zhou, Q.; Carroll, P. J.; Swager, T. M. *J. Org. Chem.* **1994**, *59*, 1294–1301.

(12) Balaban, A. T.; Banciu, M.; Ciorba, V. *Annulenes, Benzo-, Hetero-, Homo-Derivatives and their Valence Isomers*; CRC Press: Boca Raton, 1987; Vols. 1–3.

(13) (a) Kondo, K.; Yasuda, S.; Tohoru, S.; Miya, M. *J. Chem. Soc., Chem. Commun.* **1995**, 55–56. (b) Sarkar, A.; Pak, J. J.; Rayfield, G. W.; Haley, M. M. *J. Mater. Chem.* **2001**, *11*, 2943–2945.

SCHEME 1. Synthetic Strategy for Super-Sized Substructure Targets



at the periphery of the rings via triyne units such as **10**, which are the origin of the outer annulene rings. While the larger decyl chains provided better enhancement to solubility than the *tert*-butyl groups, the solubilities of the two- and three-ringed systems were still relatively poor. To combat the anticipated amplification of solubility problems associated with the larger macrocycles **3–7**, several additional groups were investigated, such as *tert*-octyl, polyether, and 3,5-di-*tert*-butylphenyl (DTBP).¹⁴ Of the three, the bulky, highly branched di-*tert*-butylphenyl unit imparted good solubility and the greatest ease in synthesis.

Syntheses. The preparation of triyne **10** began with attachment of the solubilizing group as 1-bromo-3,5-di-*tert*-butylbenzene (**11**),¹⁵ which was converted to its respective boronic ester and subsequently cross-coupled with 1-bromo-4-nitrobenzene (Scheme 2).¹⁶ Reduction of

the resultant nitrobiphenyl gave amine **12**, followed by iodination with $\text{BnEt}_3\text{N}^+ \text{ICl}_2^-$ to afford **13** in 88% yield.¹⁷ Conversion of the amino group to a piperidinyltriazene by means of diazonium chemistry provided **14** (89%).¹⁸ Sonogashira cross-coupling of **14** with trisopropylsilylacetylene (TIPSA) gave **15**, which was treated with MeI at 140 °C, converting the triazene moiety the iodide in **16**.¹⁸ A final cross-coupling of trimethylsilylbutadiyne (TMSB) afforded triyne **10** in 55% overall yield for the seven steps.

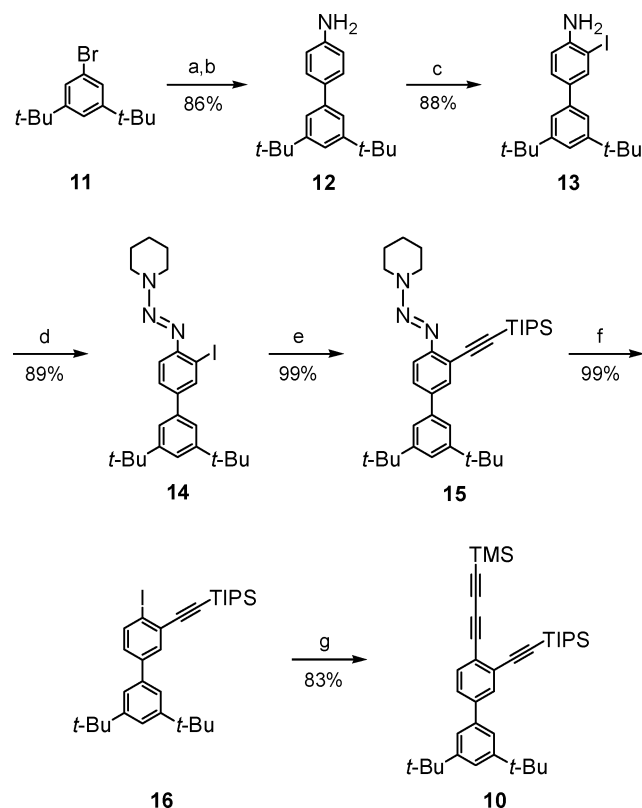
(15) Although commercially available, it is considerably less expensive to prepare **11** from 1,3,5-tri-*tert*-butylbenzene, which is also commercially available. See: Bartlett, P. D.; Roha, M.; Stiles, R. M. *J. Am. Chem. Soc.* **1954**, *76*, 2349–2351.

(16) Klein, M.; Erdinger, L.; Boche, G. *Mutat. Res.* **2000**, *467*, 69–82.

(17) Kajigaeshi, S.; Kakinami, T.; Yamasaki, H.; Fujisaki, S.; Okamoto, T. *Bull. Chem. Soc. Jpn.* **1988**, *61*, 600–603.

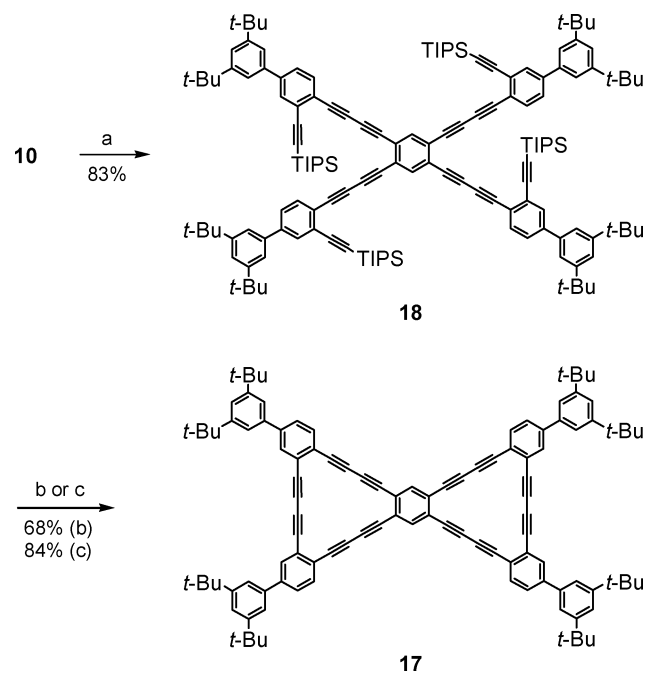
(18) Moore, J. S.; Weinstein, E. J.; Wu, Z. *Tetrahedron Lett.* **1991**, *32*, 2465–2466.

(14) Marsden, J. A. Ph.D. Thesis, University of Oregon, 2005.

SCHEME 2^a

^a Reagents and conditions: (a) [i] *t*-BuLi, (*i*-PrO)₃B, Et₂O, THF, -100 °C to room temperature, [ii] 1-bromo-4-nitrobenzene, NaOEt, Pd(PPh₃)₄, PhMe, H₂O, reflux; (b) Sn, HCl, EtOH, H₂O, reflux; (c) BnEt₃N⁺ICl₂⁻, CaCO₃, CH₂Cl₂, MeOH; (d) [i] HCl, NaNO₂, CH₃CN, THF, H₂O, -10 °C, [ii] piperidine, K₂CO₃, CH₃CN, H₂O, -10 °C to room temperature; (e) TIPSA, Pd(PPh₃)₄, CuI, *i*-Pr₂NH, THF, 40 °C; (f) MeI, 140 °C; (g) TMSB, Pd(PPh₃)₄, CuI, *i*-Pr₂NH, THF, 40 °C.

To test the effectiveness of the DTBP solubilizing group, bis[18]annulene **17** was synthesized to directly compare its solubility with that of its previously reported analogue functionalized with *n*-decyl groups.⁷ Triyne **10** was desilylated and cross-coupled to 1,2,4,5-tetraiodobenzene in an excellent 83% yield (96% for each transformation) providing α,ω -polyynes **18** (Scheme 3). The TIPS groups on precursor **18** were removed with TBAF, and the polyynes were subjected to pseudo-high dilution Cu-mediated cyclization conditions to give DBA **17** in 68% yield.¹⁹ By using a Pd-catalyzed procedure for homocoupling under similar pseudo-high dilution, which we recently reported for the preparation of bis[14]- and bis[15]annulenes,²⁰ we were able to increase the cyclization yield to a respectable 84%. Another benefit of the Pd-catalyzed route is in the ease of workup and purification, which typically involves concentration of the reaction mixture and filtration with washes of hexanes/CH₂Cl₂ to give the bright yellow DBAs that rarely needed further purification. The major drawbacks of the Cu/pyridine route include removal and use of pyridine as a solvent and the large excess of Cu salts, typically requiring

SCHEME 3^a

^a Reagents and conditions: (a) 1,2,4,5-tetraiodobenzene, KOH (aq), Pd(PPh₃)₄, CuI, *i*-Pr₂NH, THF, 50 °C; (b) [i] TBAF, THF, [ii] CuCl, Cu(OAc)₂, pyridine, 60 °C; (c) [i] TBAF, THF, [ii] Pd(dppe)Cl₂, CuI, I₂, *i*-Pr₂NH, THF, 50 °C.

filtration through silica gel to which many of the larger macrocycles are either unstable or have solubilities too poor to be carried through in the filtrate.

With bis[18]annulene **17** in hand we tested its solubility in CH₂Cl₂ at room temperature against its *n*-decyl analogue. To our chagrin, we found that the **17** was somewhat less soluble (35 vs 55 μ M), although the DTBP groups do provide other benefits such as enhancement of the optical emission and absorption characteristics due to increased conjugation. Most of the DTBP precursors were also solids rather than the thick oils characteristic of the decyl-substituted polyynes, allowing ease in handling and isolation. We therefore decided to continue the syntheses of the larger graphdiyne substructures using the 3,5-di-*tert*-butylphenyl groups for solubility.

The synthesis of asymmetrically substituted arene **9**, needed for construction of key piece **8**, starts from known 1,2-diiodo-4,5-dinitrobenzene (**19**, Scheme 4).²¹ Using NH₃ gas, substitution of one nitro group with an amino group gave aniline **20**.^{21,22} The amino group was then converted to a bromide through a diazotization affording **21**,²³ which was reduced to aniline **22**. Diazotization of **22** followed by quenching with HNMe₂ furnished multigram quantities of triazine **9** in 71% yield for the four steps.

The synthesis of polyynes **8** continued with the convergent cross-coupling of triyne **10** and arene **9** (Scheme 5). Because of the characteristic instability of terminal phenylbutadiynes, especially when concentrated, deprotection and cross-coupling of trimethylsilylbutadiynes are

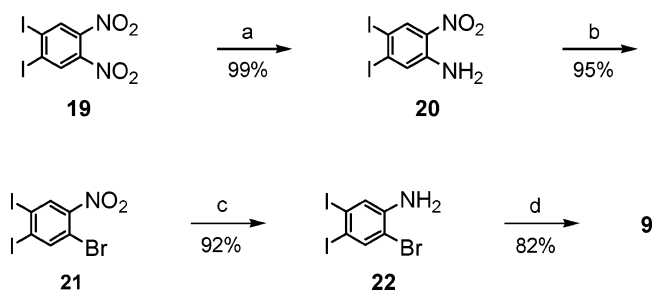
(19) Siemsen, P.; Livingston, R. C.; Diederich, F. *Angew. Chem., Int. Ed.* **2000**, *39*, 2632–2657.

(20) (a) Marsden, J. A.; Miller, J. J.; Haley, M. M. *Angew. Chem., Int. Ed.* **2004**, *43*, 1694–1697. (b) Marsden, J. A.; Miller, J. J.; Shirtcliff, L. D.; Haley, M. M. *J. Am. Chem. Soc.* **2005**, *127*, 2464–2476.

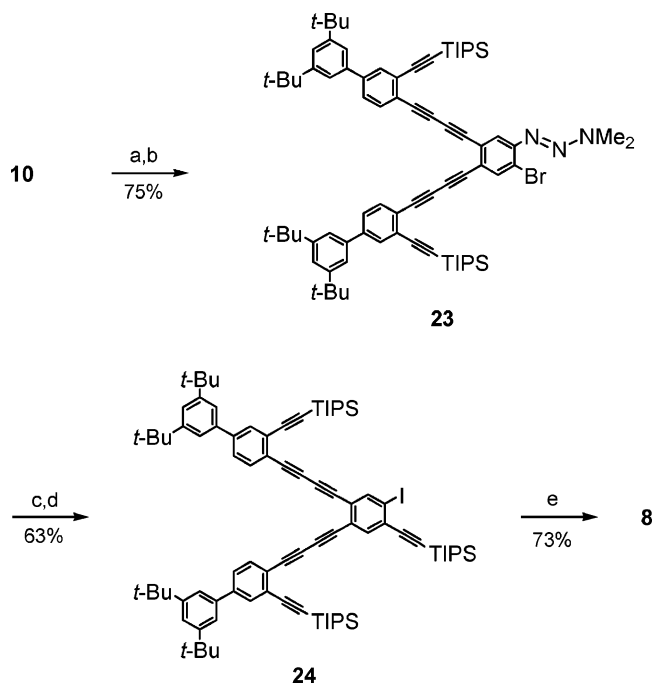
(21) Arotzky, J.; Butler, R.; Darby, A. C. *J. Chem. Soc.* **1970**, 109, 5478–5486.

(22) Senskey, M. D.; Bradshaw, J. D.; Tessier, C. A.; Youngs, W. J. *Tetrahedron Lett.* **1995**, *36*, 6217–6220.

(23) Doyle, M. P.; Siegfried, B.; J. F. Dellaria, J. *J. Org. Chem.* **1977**, *42*, 2426–2431.

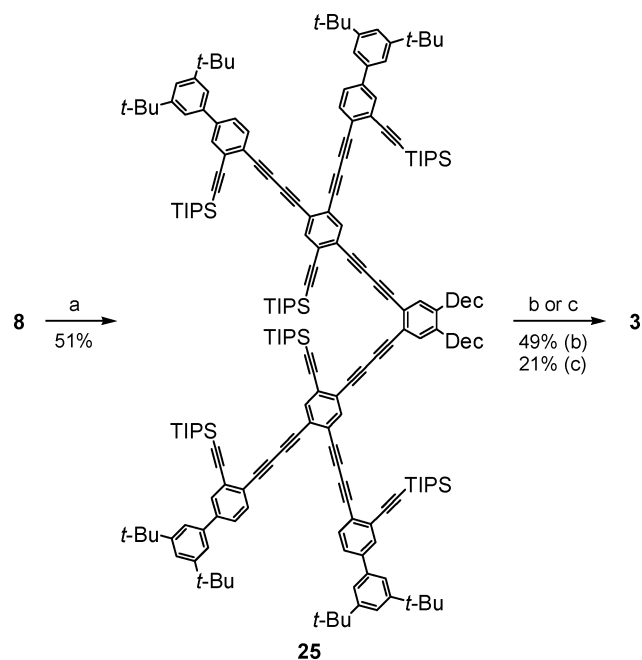
SCHEME 4^a

^a Reagents and conditions: (a) NH_3 , THF; (b) $t\text{-BuONO}$, CuBr_2 , CH_3CN , 60°C ; (c) $\text{FeSO}_4 \cdot 7\text{H}_2\text{O}$, NH_4OH , 80°C ; (d) [i] HCl , NaNO_2 , CH_3CN , THF, H_2O , -10°C , [ii] Me_2NH , K_2CO_3 , CH_3CN , H_2O , -10°C to room temperature.

SCHEME 5^a

^a Reagents and conditions: (a) K_2CO_3 , THF, MeOH; (b) **9**, $\text{Pd}(\text{PPh}_3)_4$, CuI , $i\text{-Pr}_2\text{NH}$, THF, 50°C ; (c) TIPS, $\text{Pd}(\text{PPh}_3)_4$, CuI , $i\text{-Pr}_2\text{NH}$, THF, 80°C ; (d) HI (aq), I_2 , CCl_4 , CH_3CN , 60°C ; (e) TMSB, $\text{Pd}(\text{PPh}_3)_4$, CuI , $i\text{-Pr}_2\text{NH}$, THF, 40°C .

typically performed in one step; however, the in situ triodesilylation/alkynylation procedure²⁴ of **9** and **10** gave a mixture of products, including elimination of the triazene and/or halides and substitution with a proton. Triyne **10** was therefore deprotected beforehand with $\text{K}_2\text{CO}_3/\text{MeOH}$. The inorganic salts were filtered off, and the solution was degassed and cross-coupled with no need to concentrate the terminal phenylbutadiyne, providing hexayne **23** in 75% yield with no detectable decomposition of the triazene or halides. A second cross-coupling with TIPS to the bromo position at elevated temperature in a sealed vessel, followed by conversion of the triazene to an iodoarene, provided iodoarene **24**. For the

SCHEME 6^a

^a Reagents and conditions: (a) 1,2-didecyl-4,5-diiodobenzene, KOH (aq), $\text{Pd}(\text{PPh}_3)_4$, CuI , $i\text{-Pr}_2\text{NH}$, THF, 50°C ; (b) [i] TBAF, THF, [ii] CuCl , $\text{Cu}(\text{OAc})_2$, pyridine, 60°C ; (c) [i] TBAF, THF, [ii] $\text{Pd}(\text{dppf})\text{Cl}_2$, CuI , I_2 , $i\text{-Pr}_2\text{NH}$, THF, 50°C .

latter step, triazene decomposition with MeI for **24** gave only degradation above 140°C , whereas below this temperature no reaction occurred. For that reason, several modifications were attempted until we found optimal conversion by reacting the triazene with HI and I_2 at 60°C for 30 min.²⁵ A final cross-coupling of **24** and trimethylsilylbutadiyne gave key piece **8** in 34% yield over the five steps.

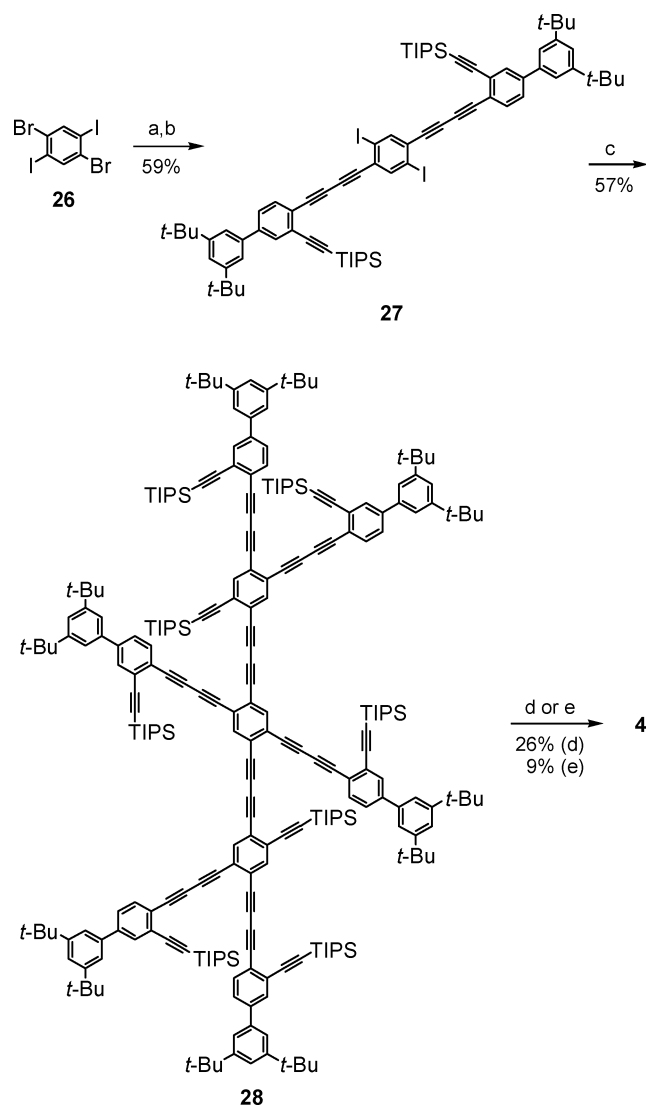
Tris[18]annulene **3** was prepared by an in situ deprotection/alkynylation of 2 equiv of key piece **8** with 1,2-didecyl-4,5-diiodobenzene,^{11d} giving acyclic precursor **25** in 51% yield (Scheme 6). After deprotection of the TIPS groups, we again performed both Cu-mediated and Pd-catalyzed cyclizations, providing graphdiyne subunit **3** as a bright yellow solid. A reversal of yields for the cyclization of this structure was seen (49% Cu, 21% Pd), although both procedures gave moderate yields for an annulenic structure of this size.

The linear conjugated pathway is further extended in "linear" tetra[18]annulene **4** to nearly 5 nm, over twice as long as any previously known graphdiyne subunit. The central core of this system was constructed by deprotection/alkynylation of 2 equiv of triyne **10** to the iodo positions of 1,4-dibromo-2,5-diiodobenzene (**26**),²⁶ followed by conversion of the remaining bromides to iodides by BuLi and I_2 in order to decrease the temperature requirements necessary for the second cross-coupling sequence (Scheme 7). Key piece **8** was next attached at the iodo positions of **27** providing **28** in 57% yield. Cyclization, after TIPS deprotection, by Cu (26%) or Pd (9%) gave tetracycle **4** as a very insoluble yellow solid.

(24) (a) Haley, M. M.; Bell, M. L.; English, J. J.; Johnson, C. A.; Weakley, T. J. R. *J. Am. Chem. Soc.* **1997**, *119*, 2956–2957. (b) Bell, M. L.; Chiechi, R. C.; Kimball, D. B.; Johnson, C. A.; Matzger, A. J.; Wan, W. B.; Weakley, T. J. R.; Haley, M. M. *Tetrahedron* **2001**, *57*, 3507–3520.

(25) Barbero, M.; Degani, I.; Diulgheroff, N.; Dughera, S.; Fochi, R. *Synthesis* **2001**, 2180–2190.

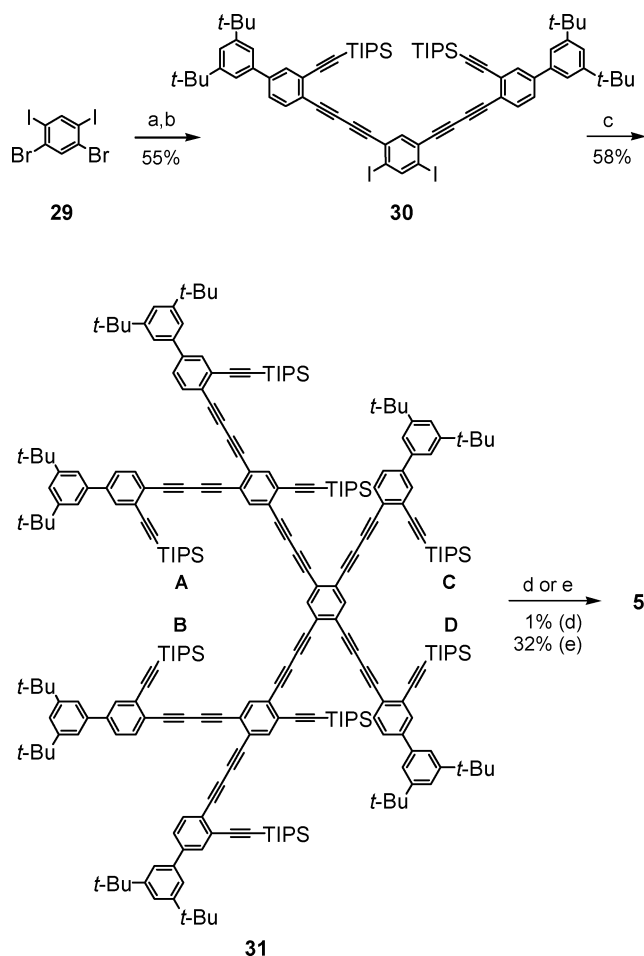
(26) Goldfinger, M. B.; Crawford, K. B.; Swager, T. M. *J. Am. Chem. Soc.* **1997**, *119*, 4578–4593.

SCHEME 7^a

^a Reagents and conditions: (a) **10**, KOH (aq), Pd(PPh₃)₄, CuI, *i*-Pr₂NH, THF, 40 °C; (b) BuLi, I₂, THF, -78 °C to room temperature; (c) **8**, KOH (aq), Pd(PPh₃)₄, CuI, *i*-Pr₂NH, THF, 55 °C; (d) [i] TBAF, THF, [ii] CuCl, Cu(OAc)₂, pyridine, 60 °C; (e) [i] TBAF, THF, [ii] Pd(dppe)Cl₂, CuI, I₂, *i*-Pr₂NH, THF, 50 °C.

Solubility for this system was estimated at ca. 0.1 μM in CH₂Cl₂ at room temperature, thus preventing characterization by NMR spectroscopy.

To compare structural isomers with different conjugated pathways, “bent” tetra[18]annulene **5** was prepared through a similar series of reactions used for DBA **4** (Scheme 8). Starting from 1,5-dibromo-2,4-diiodobenzene (**29**),²⁶ triyne cross-coupling and bromide-iodide conversion gave the central piece **30** (55%). A second series of cross-couplings with **8** gave precursor **31**, which was again deprotected and cyclized by Cu or Pd procedures. Less than 1% of tetra[18]annulene **5** was isolated after Cu-mediated cyclization along with copious amount of oligomeric material. The most likely explanation for this occurrence is intramolecular coupling across alkynes **A** and **B**, which are in close enough proximity to each other to bridge through the bis(Cu-acetylide) intermediate,^{19,27} forming a 33-membered ring. In turn, this undesirable ring formation would force the adjacent alkynes to

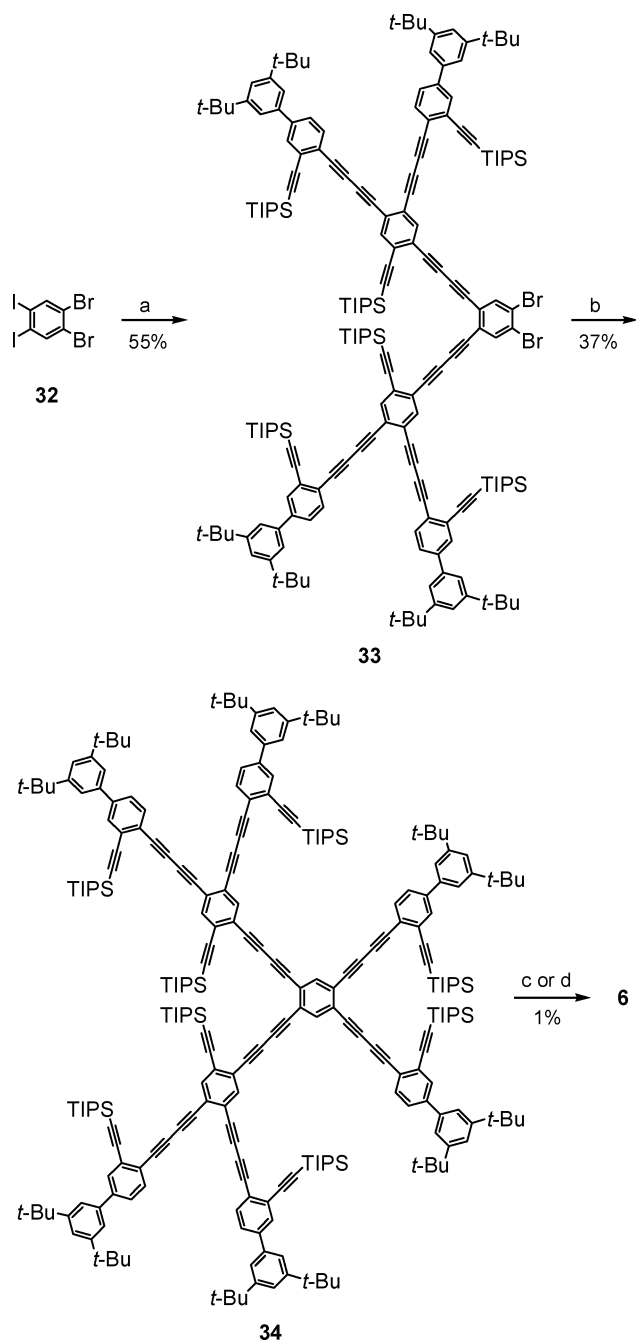
SCHEME 8^a

^a Reagents and conditions: (a) **10**, KOH (aq), Pd(PPh₃)₄, CuI, *i*-Pr₂NH, THF; (b) BuLi, I₂, THF, -78 °C to room temperature; (c) **8**, KOH (aq), Pd(PPh₃)₄, CuI, *i*-Pr₂NH, THF, 55 °C; (d) [i] TBAF, THF, [ii] CuCl, Cu(OAc)₂, pyridine, 60 °C; (e) [i] TBAF, THF, [ii] Pd(dppe)Cl₂, CuI, I₂, *i*-Pr₂NH, THF, 50 °C.

intermolecularly couple, forming the oligomeric material. Although alkynes **C** and **D** are also separated by a comparable distance, formation of the resultant 19-membered ring would be improbable because of the high ring strain associated with this size cycle. A much higher yield of 32% was achieved via Pd-catalyzed cyclization, likely attributable to the geometry about the Pd center. Using a *cis*-bidentate ligand, 1,2-bis(diphenylphosphino)ethane (dppe), addition of the acetylides to Pd must transpire in a *cis*-orientation that is unlikely between alkynes **A** and **B** and much more facile for formation of the desired 18-membered rings.²⁰ Upon formation, we found that the bent tetra[18]annulene isomer **5** was much more soluble than isomer **4** at 8 μM in CH₂Cl₂ at room temperature, likely as a result of the reduction in size across the macrocycle and/or lower symmetry.

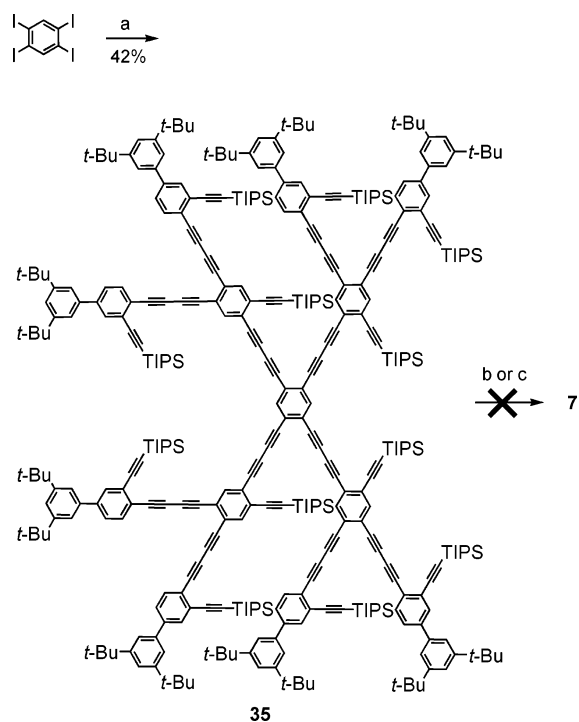
The “star-shaped” tetra[18]annulene **6** is also made up of four graphdiyne subunits and possesses an interesting *D*_{3h} symmetry with three linear “hexayne” chromophores. A modification from the syntheses of the previous DBAs was necessary for **6** due to the likelihood of benzyne

(27) Bohlmann, F.; Schönowsky, H.; Inhoffen, E.; Grau, G. *Chem. Ber.* **1963**, *97*, 794–800.

SCHEME 9^a

^a Reagents and conditions: (a) **8**, KOH (aq), Pd(PPh₃)₄, CuI, *i*-Pr₂NH, THF, 45 °C; (b) **10**, KOH (aq), Pd(PPh₃)₄, CuI, *i*-Pr₂NH, THF, reflux; (c) [i] TBAF, THF, [ii] CuCl, Cu(OAc)₂, pyridine, 60 °C; (d) [i] TBAF, THF, [ii] Pd(dppe)Cl₂, CuI, I₂, *i*-Pr₂NH, THF, 50 °C.

formation in the lithiation step of the *o*-dibromoarene. The less stable alkyne coupling piece **8** was first deprotected in situ and cross-coupled to the iodo positions of 1,2-dibromo-4,5-diiodobenzene,²⁸ (**32**) providing dibromo precursor **33** in 55% yield (Scheme 9). A second in situ deprotection/alkynylation of triyne **10** with **33** at elevated temperature gave the precyclized polyynes **34** (37%). Cyclization of this compound under both Pd-catalyzed

SCHEME 10^a

^a Reagents and conditions: (a) 1,2,4,5-tetraiodobenzene, KOH (aq), Pd(PPh₃)₄, CuI, *i*-Pr₂NH, THF, 55 °C; (b) [i] TBAF, THF, [ii] CuCl, Cu(OAc)₂, pyridine, 60 °C; (c) [i] TBAF, THF, [ii] Pd(dppe)Cl₂, CuI, I₂, *i*-Pr₂NH, THF, 50 °C.

and Cu-mediated conditions resulted in an abundant amount of oligomeric material and ~1% of macrocycle **6**, although providing enough material for analysis of its electronic properties.

Multiple attempts at the construction of the largest planned substructure, hexa[18]annulene **7**, from its precursor **35** (made by tetra-coupling of **8** with 1,2,4,5-tetraiodobenzene) were unsuccessful (Scheme 10). Despite modifications to the cyclization conditions, such as addition time, temperature, and concentration, only dark, oligomeric material resulting from intermolecular alkyne couplings was isolated. This result is not surprising, because of the size of the desired DBA system and the number of simultaneous intramolecular homocouplings necessary for product formation.

Properties. All graphdiyne subunits prepared were isolated as bright yellow, microcrystalline solids. As expected, their solubilities were increasingly poor as the overall size of the systems increased. Most notable was the very poor solubility of macrocycle **4**, with the largest calculated end-to-end distance of greater than 5 nm. In this macrocycle we have most likely reached the feasible size limit for solubility that the 3,5-di-*tert*-butylphenyl groups can adequately provide.

All annulenic (excluding **4** and **6**) and intermediate structures were fully characterized spectroscopically. Consistent with our previous studies on smaller dehydrobenzo[18]annulene graphdiyne substructures,^{7,10} a weak aromatic ring current arising from the multiple $[4n + 2]$ π -electron circuits present in each 18-membered ring was discernible based on comparison of the ¹H NMR spectra of the annulenes and the α,ω -polyynes intermediates. In each case, a distinct downfield shift ($\Delta\delta = 0.25\text{--}0.30$

(28) Miljanic, O. S.; Vollhardt, K. P. C.; Whitener, G. D. *Synlett* **2003**, 29–34.

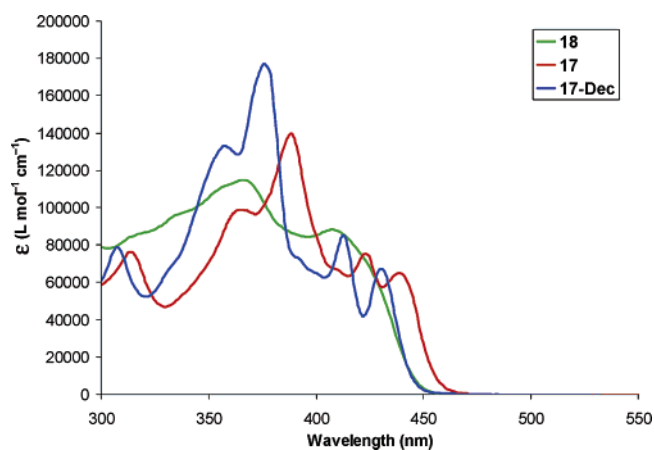


FIGURE 1. Electronic absorption spectra of precursor **18**, macrocycle **17**, and the *n*-decyl analogue of **17**.

ppm) of the interannulenic aromatic protons of the DBAs from their respective precursors was observed, indicating the presence of weak diatropic ring currents.

Of the predicted materials properties of the network graphdiyne and its subunits, the optical absorption and emission as well as NLO properties are the most readily observable and arguably of greatest interest for electrooptical devices. Each graphdiyne subunit shows a characteristic pattern of three major low-energy peaks from which much information can be gathered from the position and intensity of these absorption bands (Figures 1–4). The interesting electronic properties presumably arise from the extended two-dimensional conjugation present in the planar DBAs. The extent of delocalization can be readily observed by bathochromic shifts in the low-energy peaks of the UV–vis spectra of each system. These low-energy peaks are generally attributed to $\pi \rightarrow \pi^*$ transitions of the HOMO to the LUMO and the associated energy is minimized by increasing delocalization. Delocalization is greatly increased upon cyclization resulting from the introduction of new chromophores in the rings, ring currents, and planarization of the entire phenylacetylene framework, which can be seen in Figures 1 and 3, where bathochromic shifts of 10–25 nm from acyclic precursor to annulene were observed. The fine vibronic structure present in the macrocyclic systems and absent in the acyclic intermediates is easily visible, appearing as multiple, tight absorption peaks rather than the broad absorption bands present in the precursors. The added conjugation from the DTBP solubilizing groups over the previously used *n*-decyl chains also provided an additional red-shift of ~ 10 nm for each of the three main absorption bands in **17** compared to its previously reported decyl analogue (Figure 1).⁷

As we^{7,10,20} and others^{3,13a,29} have shown, bathochromic shifts in neutral- and donor-substituted phenylacetylene systems are maximized by linear conjugation, taking advantage of both length and the number of linear

TABLE 1. Selected Peaks from the Electronic Absorption Spectra of Macrocycles **2–6** and **17**

DBA	peak 1 ^a	peak 2 ^a	peak 3 ^a	<i>n</i> ^b
2 ^c	330 (72,000)	360 (21,000)	380 (24,000)	1
17	388 (139,000)	423 (76,000)	439 (65,000)	2
3	392 (256,000)	434 (180,000)	454 (130,000)	3
4	398 (391,000)	438 (311,000)	462 (263,000)	4
	407	454	485	∞ ^d
5	394 (301,000)	409 (299,000)	447 (242,000)	3
6	415 (264,000)	428 (204,000)	448 (295,000)	3

^a Peak values are in nm with molar absorptivity ($M^{-1} cm^{-1}$).
^b *n* = the number of phenylbutadiyne units in the longest linear conjugated pathway. ^c Reference 7. ^d Calculated from Figure 3.

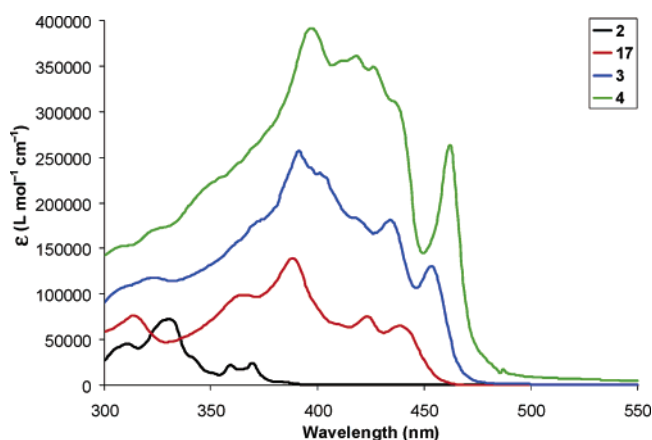


FIGURE 2. Electronic absorption spectra of graphdiyne substructures **2–4** and **17**.

chromophores present.³⁰ This trend continues with macrocycles **17**, **3**, and **4**. As each additional ring is fused onto the system in a zigzag pattern, the linearly conjugated pathway is extended by one phenylbutadiyne unit. With increasing linear conjugation, the low-energy absorption peaks (peaks 1–3, Table 1) undergo a dramatic rise in molar absorptivity (ϵ) and further bathochromic shift (Figure 2). The magnitude of these bathochromic shifts, however, decreases with each successively fused phenylbutadiyne unit (*n*), indicating saturation ($\Delta\lambda_{\max}/\Delta n = 0$) of the longest-wavelength λ_{\max} is occurring. Similar saturations have been observed for linear polyynes.³¹ The saturation wavelength can be calculated by plotting $1/n$ vs the longest-wavelength λ_{\max} , which gives a linear fit for DBAs **3**, **4**, and **17** ($n = 2–4$, Figure 3). Extrapolating for $n = \infty$ predicts a saturation point of 485 nm (2.56 eV) for λ_{\max} , which represents the HOMO–LUMO energy gap of an infinite zigzag pattern of graphdiyne subunits fused in a linear fashion such as in substructures **17**, **3**, and **4**. A much lower value of only 0.53 eV has been calculated for the band-gap energy of the entire graphdiyne network by Narita et al.¹² Subunit **4**, possessing the longest linear conjugated pathway of

(30) Meier, H.; Mühling, B.; Kolshorn, H. *Eur. J. Org. Chem.* **2004**, 1033–1042.

(31) Inter alia: (a) Johnson, T. R.; Walton, D. R. M. *Tetrahedron* **1972**, *28*, 5221–5230. (b) Dembinski, R.; Bartik, T.; Bartik, B.; Jaeger, M.; Gladysz, J. A. *J. Am. Chem. Soc.* **2000**, *122*, 810–818. (c) Gibtner, T.; Hampel, F.; Gisselbrecht, J. P.; Hirsch, A. *Chem. Eur. J.* **2002**, *8*, 408–432. (d) Luu, T.; Elliott, E.; Slepkov, A. D.; Eisler, S.; McDonald, R.; Hegmann, F. A.; Tykwinski, R. R. *Org. Lett.* **2005**, *7*, 51–54. (e) Eisler, S.; Slepkov, A. D.; Elliott, E.; Luu, T.; McDonald, R.; Hegmann, F. A.; Tykwinski, R. R. *J. Am. Chem. Soc.* **2005**, *127*, 2666–2676.

(29) (a) Tykwinski, R. R.; Schreiber, M.; Carlon, R. P.; Diederich, F.; Gramlich, V. *Helv. Chim. Acta* **1996**, *79*, 2249–2280. (b) Tykwinski, R. R.; Schreiber, M.; Gramlich, V.; Seiler, P.; Diederich, F. *Adv. Mater.* **1996**, *8*, 226–31. (c) Wilson, J. N.; Smith, M. D.; Enkelmann, V.; Bunz, U. H. F. *Chem. Commun.* **2004**, 1700–1701. (d) Wilson, J. N.; Josowicz, M.; Wang, Y.; Bunz, U. H. F. *Chem. Commun.* **2003**, 2962–2963.

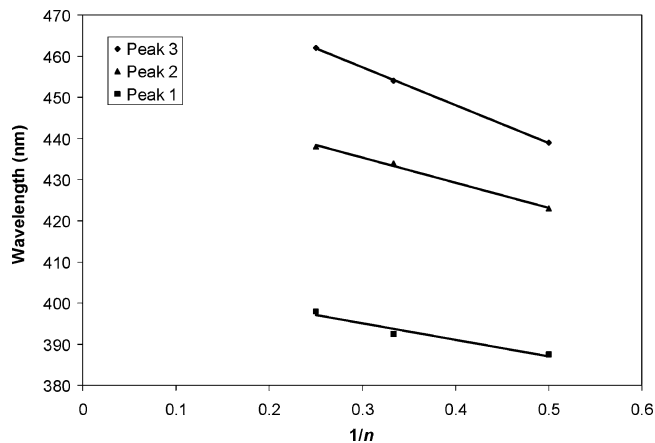


FIGURE 3. Plot of λ_{\max} versus $1/n$ for the low-energy peaks of DBAs **3**, **4**, and **17**, where n = the number of phenylbutadiyne units in the longest linear conjugated pathway.

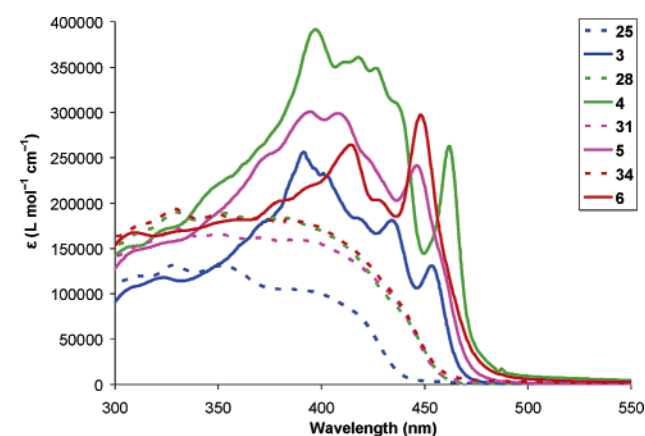


FIGURE 4. Electronic absorption spectra of graphdiyne substructures **3–6** and their acyclic precursors.

any reported annulenic structure, is only 24 nm (0.13 eV) from the predicted saturation value, suggesting that further extension of the pathway would provide little enhancement to the optical properties. The saturation wavelengths of absorption peaks 1 and 2 were similarly calculated and are reported in Table 1.

To gain further insight into the influence of the number and length of linear conjugated pathways on the elec-

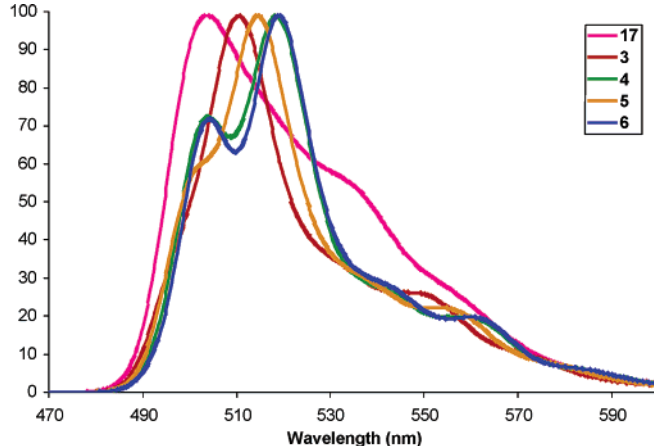
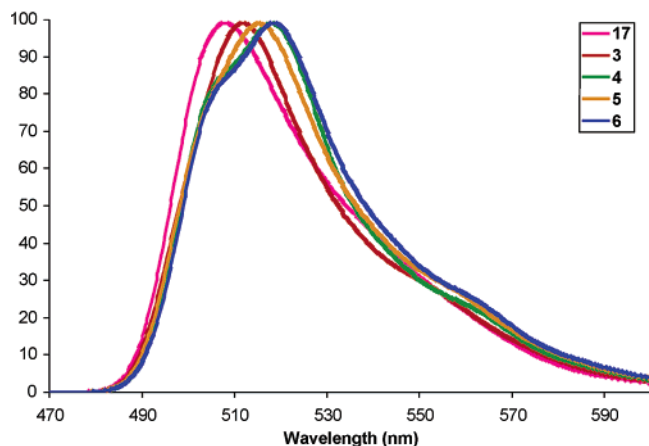


FIGURE 5. Optical emission spectra of graphdiyne substructures **3–6** and **17** in CH_2Cl_2 (left) and PhMe (right). The y-axis scale has been normalized.

tronic absorption wavelength and molar absorptivity, UV–vis spectra of tris[18]annulene **3** and tetra[18]annulene isomers **4–6** were compared. Structures **3**, **5**, and **6** all possess a longest, linear-conjugated pathway of $n = 3$ and show little variance in the wavelength of the lowest-energy λ_{\max} of 454, 447, and 448 nm, respectively (Figure 4, Table 1); however, a striking difference is observed in their molar absorptivities, which increase dramatically with the number of $n = 3$ pathways present in the macrocycle (one in **3**, two in **5**, and three in **6**). Tetra[18]annulene **4**, with no $n = 3$ linear conjugated pathway but one $n = 4$ pathway, displays a red-shift of the lowest-energy λ_{\max} from **3**, **5**, and **6** of ~ 15 nm and a value of ϵ between that of **5** and **6**. These data indicate that the wavelength, or HOMO–LUMO band-gap energy, is dictated more by the length of the longest linear conjugated pathway, whereas the molar absorptivity is dictated more by the number of long pathways present.

Each macrocycle and its acyclic precursor are also quite fluorescent, and their solution-based emission was measured in CH_2Cl_2 and PhMe (Figure 5 and Table 2). The increased conjugation due to planarization and cyclization generally resulted in an increase of 2–3 times the quantum efficiency to 30–60% and a slight bathochromic shift of the emission λ_{\max} . Solvent polarity showed little effect on quantum yield between CH_2Cl_2 and PhMe, although a variance in peak structure was observed. For the most part, only one broad emission band was seen in CH_2Cl_2 , while fine structure was more pronounced for the larger macrocycles in PhMe with at least three individual peaks observable for tetra[18]annulenes **4–6**. As with the absorption spectra, increasing the number of long linear chromophores had a pronounced effect on the emission spectra of the graphdiyne substructures. With macrocycles **3**, **5**, and **6**, as the number of $n = 3$ pathways increased, a quantum efficiency increase of $\sim 10\%$ and a bathochromic shift of ~ 5 nm resulted from each additional pathway. Comparatively, DBA **4**, containing a longer $n = 4$ conjugated pathway, showed an emission spectrum only slightly hypsochromically shifted from that of **6**. These data indicate that for emission properties in the graphdiyne substructures, three $n = 3$ pathways behave similarly to one $n = 4$.

Macrocycles **3–6** and **17** proved to be air-stable over a period of several months and much more robust to

TABLE 2. Optical Emission Data for Macrocycles 3–6 and 17 and Their Acyclic Precursors

compound	solvent	λ_{em}^a	Stokes shift ^a	Φ_p^b
18	CH ₂ Cl ₂	508	79	0.13
	PhMe	507	85	0.11
17	CH ₂ Cl ₂	508	67	0.25
	PhMe	504	65	0.25
25	CH ₂ Cl ₂	510	86	0.08
	PhMe	512	94	0.09
3	CH ₂ Cl ₂	512	53	0.31
	PhMe	510	57	0.32
28	CH ₂ Cl ₂	509	65	0.17
	PhMe	507	67	0.17
4	CH ₂ Cl ₂	518	58	0.40
	PhMe	518, 504	57	0.30
31	CH ₂ Cl ₂	509	67	0.20
	PhMe	506	66	0.17
5	CH ₂ Cl ₂	514	66	0.61
	PhMe	514, 502	67	0.42
34	CH ₂ Cl ₂	510	70	0.21
	PhMe	507	67	0.19
6	CH ₂ Cl ₂	519	72	0.52
	PhMe	519, 504	70	0.49
35	CH ₂ Cl ₂	510	67	0.22
	PhMe	510	67	0.22

^a Values are in nm. ^b With reference to fluorescein.

temperature than their acyclic precursors. Decomposition to a black, insoluble material occurred at relatively high temperatures of 200–250 °C, resulting in a broad exotherm as measured by DSC, indicative of random polymerization/degradation, whereas most acyclic precursors showed similar decomposition around 150–170 °C.

Conclusions

We have demonstrated the synthesis of increasingly larger substructures (3–6) of the network graphdiyne (2) through the use of convergent syntheses taking advantage of three key pieces, nonayne 8, arene 9, and triyne 10, in conjunction with several modifications to the Sonogashira cross-coupling protocol and intramolecular homocoupling via Cu or Pd to affect ring closure. Incorporation of 3,5-di-*tert*-butylphenyl groups to the periphery of the macrocycles provided both increased solubility and enhancement of the optical properties. Electronic absorption spectra indicate a reliance of the longest-wavelength absorption on the length of linear conjugation and saturation of this peak shifting has nearly been reached with macrocycle 4. A relationship was also established between the number of long linear conjugated pathways and an increase in molar absorptivity with values approaching 400,000 M⁻¹ cm⁻¹, more than double any previously measured value for dehydrobenzoannulene systems. Similar dependencies on chromophore length and number were observed in the optical emission spectra of 3–6. Currently under investigation are the origins of the excitation properties of all graphdiyne substructures, which will be reported in due course.

Experimental Section

General Methods. ¹H and ¹³C NMR spectra were recorded in CDCl₃ or CD₂Cl₂ using a 300 (¹H, 299.94 MHz; ¹³C, 75.43 MHz) or 500 (¹H, 500 MHz; ¹³C, 125 MHz) MHz spectrometer. Chemical shifts (δ) are expressed in ppm relative to the residual CHCl₃ (¹H, 7.26 ppm; ¹³C, 77.0 ppm) reference.

Coupling constants are expressed in hertz. Melting points were recorded on a melting point apparatus in open-end capillary tubes or on a DSC in air and are uncorrected. IR spectra were recorded using an FTIR spectrometer. UV–vis spectra were recorded on a UV–vis spectrophotometer. Mass spectra were recorded on an LC/MSD spectrometer. THF and Et₂O were purified by a solvent purification system. All other chemicals were of reagent quality and used as obtained from manufacturers. Column flash chromatography was performed using N₂ or air pressure on silica gel (230–450 mesh). Precoated silica gel plates (200 × 200 × 0.50 mm) were used for analytical thin-layer chromatography. Eluting solvents were reagent quality and used as obtained from the manufacturers. Reactions were carried out in an inert atmosphere (dry Ar) when necessary. All deprotected terminal alkynes were used directly without further purification.

General Alkyne Cross-Coupling Procedure A. Haloarene (1 equiv) and terminal alkyne, if solid or viscous oil (addition of liquid alkynes occurred via injection after Ar purge) (1.1 equiv per transformation), were dissolved in *i*-Pr₂NH/THF (1:1, ~0.1 M) in a round-bottom flask. The solution was purged for 30 min with bubbling Ar followed by addition of Pd(PPh₃)₄ (0.03 equiv per transformation) and CuI (0.06 equiv per transformation). The reaction mixture then stirred at room temperature to 80 °C for 2–12 h under an Ar atmosphere. Upon completion, the mixture was concentrated, rediluted with CH₂Cl₂, and filtered through a plug of silica gel. The solvent was removed in vacuo and the crude material was purified by column chromatography.

General in Situ Deprotection/Alkynylation Procedure B. Haloarene (1 equiv) was dissolved in *i*-Pr₂NH/THF (1:1, ~0.01 M) in a round-bottom flask. To this solution was added KOH (10 equiv per alkyne) dissolved in a minimal amount of H₂O. The mixture was purged for 30 min with bubbling Ar followed by addition of Pd(PPh₃)₄ (0.03 equiv per transformation) and CuI (0.06 equiv per transformation). A solution of alkyne (1.1 equiv per transformation) in THF (0.05 M) was similarly purged with Ar and added to the haloarene solution via syringe over 8–24 h. The reaction mixture then stirred at room temperature to 60 °C for 2–12 h under an Ar atmosphere. Upon completion, the mixture was concentrated, rediluted with CH₂Cl₂, and filtered through a plug of silica gel. The solvent was removed in vacuo and the crude material was purified by column chromatography.

General Cu-Mediated Cyclization Procedure C. To a solution of triisopropylsilyl-protected alkyne (1 equiv) in THF (~0.2 M) was added TBAF (1 M in THF, 5 equiv per silyl group). The reaction mixture stirred at room temperature for 15 min. Upon completion, the mixture was diluted with Et₂O, washed with brine (4×) and H₂O, dried (MgSO₄), and concentrated in vacuo. The resultant terminal alkyne was then redissolved in pyridine (50 mL) and added via syringe pump over 24 h to a suspension of Cu(OAc)₂ (20 equiv) and CuCl (25 equiv) in pyridine/MeOH (7:1, ~3 L per mmol alkyne) at 60 °C open to air. Upon completion of the slow addition, the reaction mixture stirred an additional 2 h. The suspension was concentrated in vacuo, resuspended in CH₂Cl₂, and filtered through a plug of silica gel. The crude annulene was then purified by either chromatography on a plug of silica gel or by trituration in hexanes/CH₂Cl₂ and filtration.

General Pd-Catalyzed Cyclization Procedure D. To a solution of triisopropylsilyl-protected alkyne (1 equiv) in THF (~0.2 M) was added TBAF (1 M in THF, 5 equiv per silyl group). The reaction mixture stirred at room temperature for 15 min. Upon completion, the solution was diluted with Et₂O, washed with brine (4×) and H₂O, dried (MgSO₄), and concentrated in vacuo. The resultant terminal alkyne was then redissolved in THF (50 mL) and added via syringe pump over 24 h to a solution of Pd(dppe)Cl₂ (0.1 equiv), CuI (0.15 equiv) and I₂ (0.5 equiv) in THF/*i*-Pr₂NH (1:1, ~2 L per mmol alkyne) at 50 °C open to air. Upon completion of the slow addition, the reaction mixture stirred an additional 2 h. The solution

was concentrated in vacuo, redissolved in CH_2Cl_2 , and filtered through a plug of silica gel. The crude annulene was then purified by either chromatography on a plug of silica gel or by trituration in hexanes/ CH_2Cl_2 and filtration.

Ethynyltriazene 15. Iodoarene **14** (13.6 g, 26.3 mmol) was reacted with TIPSAs (5.29 g, 29.0 mmol) at 40 °C using general alkyne cross-coupling procedure A (8 h). The crude material was purified on a plug of silica gel (1:1 CH_2Cl_2 /hexanes) to give **15** (14.9 g, 99%) as an amorphous, yellow solid: mp 84–86 °C; ^1H NMR (300 MHz, CDCl_3) δ 7.69 (d, $J = 1.8$ Hz, 1H), 7.53 (d, $J = 8.4$ Hz, 1H), 7.47 (dd, $J = 8.4, 1.8$ Hz, 1H), 7.43 (t, $J = 1.8$ Hz, 1H), 7.41 (d, $J = 1.8$ Hz, 2H), 3.86 (br s, 4H), 1.72 (br s, 6H), 1.39 (s, 18H), 1.16 (s, 21H); ^{13}C NMR (75 MHz, CDCl_3) δ 151.2, 151.1, 139.8, 139.2, 132.4, 128.2, 121.41, 121.38, 118.8, 117.0, 105.3, 94.3, 35.0, 31.5, 24.4, 22.3, 18.7, 14.3, 11.4; IR (KBr) ν 3421, 2942, 2863, 2151, 1425, 1362, 1191, 1102, 678 cm^{-1} ; MS (APCI) m/z (%) 558.4 ($\text{M} + \text{H}^+$, 100), 517.3 (10), 473.4 (40).

Ethynylbiphenyl 16. Triazene **15** (15.0 g, 26.2 mmol) in MeI (125 mL) was heated at 140 °C in a sealed pressure vessel for 12 h. Upon completion, the mixture was cooled to room temperature and concentrated in vacuo. The residue was redissolved in CH_2Cl_2 , filtered through a plug of silica gel, and concentrated in vacuo. The crude material was purified on a plug of silica gel (3:1 hexanes/ CH_2Cl_2) to give **16** (15.3 g, 99%) as a thick, yellow oil: ^1H NMR (300 MHz, CDCl_3) δ 7.89 (d, $J = 8.4$ Hz, 1H), 7.66 (d, $J = 1.8$ Hz, 1H), 7.47 (t, $J = 1.8$ Hz, 1H), 7.35 (d, $J = 1.8$ Hz, 2H), 7.20 (dd, $J = 8.4, 1.8$ Hz, 1H), 1.39 (s, 18H), 1.19 (s, 21H); ^{13}C NMR (75 MHz, CDCl_3) δ 151.4, 142.4, 139.0, 138.9, 132.1, 130.3, 128.7, 122.0, 121.4, 108.1, 99.1, 95.3, 35.0, 31.5, 18.7, 11.3; IR (KBr) ν 2961, 2865, 2156, 1730, 1363, 678 cm^{-1} ; MS (APCI) m/z (%) 595.3 ($\text{M}^+ + \text{Na}$, 20), 525.3 (20), 509.3 (70), 477.3 (95), 312.8 (100).

Triyne 10. Iodoarene **16** (5.87 g, 10.0 mmol) was reacted with trimethylsilyl-1,3-butadiyne (2.30 g, 18.8 mmol) at 40 °C using general alkyne cross-coupling procedure A (12 h). The crude material was purified by column chromatography (50:1 hexanes/ CH_2Cl_2) to give **10** (4.82 g, 83%) as an amorphous, yellow solid: mp 70–72 °C; ^1H NMR (300 MHz, CDCl_3) δ 7.65 (d, $J = 1.8$ Hz, 1H), 7.54 (d, $J = 8.4$ Hz, 1H), 7.47 (t, $J = 1.8$ Hz, 1H), 7.46 (dd, $J = 8.4, 1.8$ Hz, 1H), 7.37 (d, $J = 1.8$ Hz, 2H), 1.38 (s, 18H), 1.19 (s, 21H), 0.25 (s, 9H); ^{13}C NMR (75 MHz, CDCl_3) δ 151.4, 143.1, 139.0, 133.0, 131.0, 127.8, 127.2, 122.9, 122.2, 121.5, 104.6, 96.0, 91.5, 88.2, 78.3, 75.4, 35.0, 31.5, 18.7, 11.3, -0.4; IR (KBr) ν 3420, 2962, 2865, 2197, 2156, 2104, 1250, 1143, 1100, 846 cm^{-1} ; MS (APCI) m/z (%) 639.4 ($\text{M}^+ + \text{THF}$, 100), 598.4 ($\text{M}^+ + \text{Na}$, 15), 567.2 ($\text{M} + \text{H}^+$, 15), 531.5 (20), 392.2 (30).

Dodecayne 18. Triyne **10** (871 mg, 1.50 mmol) was reacted with 1,2,4,5-tetraiodobenzene (194 mg, 0.333 mmol) at 50 °C using general in situ deprotection/alkynylation procedure B (10 h injection, 8 h additional heating). The crude material was purified by column chromatography (20:1–7:1 hexanes/ CH_2Cl_2) to give **18** (578 mg, 83%) as a yellow solid: mp 150–153 °C; ^1H NMR (300 MHz, CDCl_3) δ 7.72 (d, $J = 1.5$ Hz, 4H), 7.68 (s, 2H), 7.67 (d, $J = 8.3$ Hz, 4H), 7.53 (dd, $J = 8.3, 1.5$ Hz, 4H), 7.50 (t, $J = 1.5$ Hz, 4H), 7.42 (d, $J = 1.5$ Hz, 8H), 1.41 (s, 72H), 1.23 (s, 84H); ^{13}C NMR (75 MHz, CDCl_3) δ 151.4, 143.4, 139.0, 137.6, 133.3, 131.1, 127.6, 127.2, 125.5, 122.9, 122.3, 121.5, 104.5, 96.4, 83.6, 81.2, 79.1, 78.0, 35.0, 31.5, 18.7, 11.3; IR (KBr) ν 2960, 2864, 2208, 2156, 1457, 668 cm^{-1} ; MS (APCI) m/z (%) 2219.1 ($\text{M}^+ + \text{THF}$, 40), 1908.6 (100), 1177.8 (50), 467.4 (20); UV (CH_2Cl_2) λ_{max} (log ϵ) 265 (5.20), 365 (5.06), 408 (4.95).

Bis[18]annulene 17. Polyyne **18** (143 mg, 0.068 mmol) was subjected to general Cu-mediated cyclization procedure C or Pd-catalyzed cyclization procedure D. The crude material was trituated with hexanes (20 mL) and filtered to give **17** (68 mg, 64% (procedure C); 84 mg, 84% (procedure D)) as a bright yellow solid: mp 200–220 °C (dec); ^1H NMR (300 MHz, CDCl_3) δ 7.95 (s, 2H), 7.93 (d, $J = 1.8$ Hz, 4H), 7.79 (d, $J = 8.1$ Hz, 4H), 7.68 (dd, $J = 8.1, 1.8$ Hz, 4H), 7.50 (t, $J = 1.5$ Hz, 4H),

7.44 (d, $J = 1.5$ Hz, 8H), 1.40 (s, 72H); ^{13}C NMR (75 MHz, CDCl_3 , 50 °C) δ 151.7, 143.5, 138.6, 136.6, 133.2, 131.5, 128.0, 126.0, 125.4, 123.4, 122.6, 121.5, 82.8, 81.3, 81.1, 79.8, 78.5, 78.3, 35.1, 31.5; IR (KBr) ν 2964, 2715, 2456, 2195, 2192, 669 cm^{-1} ; MS (APCI) m/z (%) 1491.7 ($\text{M}^+ + \text{THF}$, 80), 1443.1 ($\text{M}^+ + \text{Na}$, 100), 1009.7 (60), 677.2 (60); UV (CH_2Cl_2) λ_{max} (log ϵ) 231 (5.03), 314 (4.88), 365 (4.99), 389 (5.14), 423 (4.88), 439 (4.81).

Hexayne 23. To a solution of triyne **10** (7.00 g, 12.0 mmol) in THF (50 mL) and MeOH (10 mL) was added K_2CO_3 (5.00 g, 36.0 mmol). After stirring at room temperature for 2 h, the mixture was filtered. The resultant terminal alkyne solution was purged with Ar for 20 min and added via syringe over 6 h to an Ar-purged solution of haloarene **9** (2.61 g, 5.44 mmol), $\text{Pd}(\text{PPh}_3)_4$ (250 mg, 0.27 mmol), and CuI (100 mg, 0.54 mmol) in THF (100 mL) and $i\text{Pr}_2\text{NH}$ (100 mL) at 50 °C under an Ar atmosphere. The mixture was stirred at 50 °C for an additional 9 h to completion, cooled to room temperature, diluted with CH_2Cl_2 (200 mL) and washed with 10% aqueous HCl until slightly acidic. The organic phase was dried (MgSO_4), filtered through a plug of silica gel, and concentrated in vacuo. The crude material was purified by column chromatography (10:1–5:1 hexanes/ CH_2Cl_2) to give **23** (4.16 g, 75%) as a yellow solid: mp 135–137 °C; ^1H NMR (300 MHz, CDCl_3) δ 7.78 (s, 1H), 7.71 (d, $J = 1.4$ Hz, 2H), 7.66 (s, 1H), 7.64 (d, $J = 8.4$ Hz, 1H), 7.63 (d, $J = 8.4$ Hz, 1H), 7.52 (dd, $J = 8.4, 1.4$ Hz, 2H), 7.49 (t, $J = 1.5$ Hz, 2H), 7.41 (d, $J = 1.5$ Hz, 4H), 3.62 (s, 3H), 3.33 (s, 3H), 1.41 (s, 36H), 1.23 (s, 21H), 1.22 (s, 21H); ^{13}C NMR (75 MHz, CDCl_3) δ 151.4 (2C), 148.3, 143.1, 143.0, 139.0 (2C), 137.7, 133.1, 133.0, 131.0 (2C), 127.6, 127.5, 127.1 (2C), 124.7, 123.3 (2C), 122.5, 122.2 (2C), 121.9, 121.5 (2C), 120.3, 104.7 (2C), 96.2, 96.1, 82.4, 82.0, 80.3, 79.8, 78.9, 78.4 (2C), 78.3, 43.4, 36.5, 35.0 (2C), 31.5 (2C), 18.7 (2C), 11.4 (2C); IR (KBr) ν 3066, 2959, 2863, 2209, 2154, 1593, 1469, 1339, 1091, 876, 832, 669 cm^{-1} ; MS (APCI) m/z (%) 1214.6 ($\text{M}^+(\text{Br}) + \text{H}^+$, 100), 1212.6 ($\text{M}^+(\text{Br}) + \text{H}^+$, 95), 1171.6 (15), 722.2 (95), 720.2 (50), 675.3 (15), 157.4 (20).

Heptayne Triazene. Hexayne **23** (4.16 g, 3.35 mmol) was reacted with TIPSAs (1.08 g, 6.00 mmol) at 80 °C in a sealed pressure vessel using general alkyne cross-coupling procedure A (16 h). The crude material was purified by column chromatography (10:1–7:1 hexanes/ CH_2Cl_2) to give the product (3.45 g, 77%) as a yellow solid: mp 136–140 °C; ^1H NMR (300 MHz, CDCl_3) δ 7.71–7.68 (m, 4H), 7.78 (s, 1H), 7.63 (d, $J = 8.4$ Hz, 2H), 7.52 (dd, $J = 8.4, 1.4$ Hz, 2H), 7.50 (t, $J = 1.5$ Hz, 2H), 7.41 (d, $J = 1.5$ Hz, 4H), 3.60 (s, 3H), 3.30 (s, 3H), 1.41 (s, 36H), 1.23 (s, 21H), 1.22 (s, 21H), 1.18 (21H); ^{13}C NMR (75 MHz, CDCl_3) δ 151.7, 151.4 (2C), 143.1, 143.0, 139.1, 139.0 (2C), 133.1, 133.0, 131.0 (2C), 127.6, 127.5, 127.1 (2C), 125.0, 123.5, 123.3, 122.3, 122.2, 121.7, 121.5 (2C), 120.8, 119.5, 104.7, (2C), 103.7, 97.7, 96.2, 96.1, 82.3, 81.9, 80.9, 80.5, 78.9, 78.6, 78.4, 78.3, 43.4, 36.5, 35.0 (2C), 31.0 (2C), 18.7 (3C), 11.4 (2C), 11.3; IR (KBr) ν 2958, 2864, 2208, 2151, 1591, 1473 cm^{-1} ; MS (APCI) m/z (%) 1314.8 ($\text{M} + \text{H}^+$, 20), 1002.5 (15), 822.4 (100), 722.2 (15).

Iodoheptayne 24. A solution of the heptayne triazene from above (3.40 g, 2.53 mmol) in CCl_4 (100 mL) was added to a solution of HI (48% aqueous, 2.20 mL, 12.5 mmol) and I_2 (3.18 g, 12.5 mmol) in CH_3CN (100 mL) at 60 °C via syringe over 30 min. The mixture was heated an additional 15 min to completion by TLC. After cooling to room temperature, the mixture was diluted with CH_2Cl_2 (100 mL) and washed successively with saturated NaHCO_3 solution (150 mL), 5% aqueous NaHSO_3 solution (150 mL), and H_2O (150 mL). The organic phase was dried (MgSO_4), filtered through a plug of silica gel, and concentrated in vacuo. The crude material was purified by column chromatography (50:1 hexanes/ CH_2Cl_2) to give **24** (2.60 g, 82%) as a red solid: mp 129.0–131.1 °C; ^1H NMR (300 MHz, CDCl_3) δ 8.00 (s, 1H), 7.68–7.66 (m, 2H), 7.61 (d, $J = 8.4$ Hz, 1H), 7.60 (d, $J = 8.4$ Hz, 1H), 7.59 (s, 1H), 7.50 (dd, $J = 8.4, 1.4$ Hz, 1H), 7.49 (dd, $J = 8.4, 1.4$ Hz, 1H), 7.47 (t, $J = 1.5$ Hz, 2H), 7.38 (d, $J = 1.5$ Hz, 4H), 1.38 (s, 36H),

1.18 (s, 42H), 1.17 (21H); ^{13}C NMR (75 MHz, CDCl_3) δ 151.4 (2C), 143.4, 143.3, 143.0, 139.0 (2C), 137.1, 133.2, 133.0, 131.1 (2C), 130.6, 127.7, 127.6, 127.2 (2C), 125.4, 124.9, 123.0, 122.9, 122.3 (2C), 121.5 (2C), 106.8, 104.6, 104.5, 100.3, 99.3, 96.4, 96.3, 83.6, 82.8, 80.9, 79.9, 79.1, 78.7, 78.0, 77.9, 35.0 (2C), 31.5 (2C), 18.7 (2C), 18.7, 11.3 (2C), 11.2; IR (KBr) ν 2959, 2864, 2213, 2146, 1593, 1465 cm^{-1} ; MS (APCI) m/z (%) 1442.7 (M^+ + THF, 30), 1369.8 ($\text{M} + \text{H}^+$, 100), 1277.8 (25), 1244.8 (20), 1031.2 (10), 225.3 (50).

Key Piece 8. Iodoarene **24** (2.50 g, 1.79 mmol) was reacted with trimethylsilyl-1,3-butadiyne (328 mg, 2.68 mmol) at 35 °C using general alkyne cross-coupling procedure A (2 h). The crude material was purified by column chromatography (33:1–20:1 hexanes/ CH_2Cl_2) to give **8** (1.81 g, 73%) as a brown solid: mp 141–145 °C; ^1H NMR (300 MHz, CDCl_3) δ 7.68 (d, $J = 1.8$ Hz, 2H), 7.62 (s, 1H), 7.61 (d, $J = 8.4$ Hz, 1H), 7.60 (d, $J = 8.4$ Hz, 1H), 7.57 (s, 1H), 7.49 (dd, $J = 8.4$, 1.8 Hz, 2H), 7.47 (t, $J = 1.5$ Hz, 2H), 7.38 (d, $J = 1.5$ Hz, 4H), 1.39 (s, 36H), 1.19 (s, 42H), 1.18 (21H), 0.25 (s, 9H); ^{13}C NMR (75 MHz, CDCl_3) δ 151.4 (2C), 143.4, 143.3, 142.4, 139.0 (2C), 137.1, 137.0, 133.2, 133.1, 131.0 (2C), 127.7, 127.66, 127.6, 127.2 (2C), 125.3, 124.7, 124.5, 122.9, 122.3 (2C), 121.5 (2C), 104.5(2C), 103.1, 99.8 (2C), 96.4, 93.5, 87.6, 83.5, 83.3, 81.1, 80.5 (2C), 79.4, 79.1, 77.9, 76.6, 73.7, 35.0 (2C), 31.5 (2C), 18.7 (2C), 18.6, 11.3 (2C), 11.2, –0.5; IR (KBr) ν 2960, 2865, 2208, 2156, 2099, 1591, 1458, 847, 668 cm^{-1} ; MS (APCI) m/z (%) 1436.8 (M^+ + THF, 30), 1363.7 ($\text{M} + \text{H}^+$, 100), 1323.7 (10), 1244.8 (10), 767.4 (10), 326.3 (20).

Tri[18]annulene Precursor 25. Key piece **8** (300 mg, 0.215 mmol) was reacted with 1,2-didecyl-4,5-diiodobenzene^{1d} (60 mg, 0.098 mmol) at 50 °C using general in situ deprotection/alkynylation procedure B (8 h injection, 4 h additional heating). The crude material was purified by column chromatography (15:1 hexanes/ CH_2Cl_2) to give **25** (149 mg, 51%) as a yellow-brown solid: mp 116–119 °C; ^1H NMR (300 MHz, CDCl_3) δ 7.66 (d, $J = 1.5$ Hz, 4H), 7.64 (s, 2H), 7.63 (s, 2H), 7.60 (d, $J = 8.4$ Hz, 2H), 7.59 (d, $J = 8.4$ Hz, 2H), 7.48 (dd, $J = 8.4$, 1.5 Hz, 4H), 7.45 (t, $J = 1.5$ Hz, 4H), 7.37 (d, $J = 1.5$ Hz, 8H), 7.34 (s, 2H), 2.60 (t, $J = 7.6$ Hz, 4H), 1.62–1.52 (m, 4H), 1.38 (s, 36H), 1.37 (s, 36H), 1.35–1.21 (m, 28H), 1.18 (s, 42H), 1.169 (s, 42H), 1.165 (s, 42H), 0.89 (t, $J = 7.6$ Hz, 6H); ^{13}C NMR (75 MHz, CDCl_3) δ 151.4, 151.3, 143.2, 143.2, 142.7, 139.0 (2C), 137.23, 137.21, 137.0, 134.3, 133.2, 133.1, 131.1 (2C), 127.7, 127.6, 127.3, 127.1 (2C), 125.4, 125.1, 124.5, 123.0, 122.3, 122.2, 122.0, 121.5 (2C), 104.6, 104.5, 103.2, 100.0, 99.9, 96.4, 83.5, 83.2, 82.4, 81.0, 80.7, 80.5, 79.8, 79.5, 79.2, 78.1, 78.0, 77.1, 35.0 (2C), 32.5, 31.9, 31.5 (2C), 30.6, 29.7, 29.6, 29.56, 29.5, 29.3, 22.7, 18.7 (3C), 14.1, 11.3 (2C), 11.3; IR (KBr) ν 2958, 2869, 2205, 2143, 1595, 1478, 836 cm^{-1} ; MS (APCI) m/z (%) 2941.5 ($\text{M} + \text{H}^+$, 20), 2884.2 (25), 1434.5 (100); UV (CH_2Cl_2) λ_{max} (log ϵ) 264 (5.27), 328 (5.12), 352 (5.12), 383 (5.02).

Tri[18]annulene 3. Acyclic precursor **25** (100 mg, 0.0340 mmol) was subjected to both general Cu-mediated cyclization procedure C and general Pd-catalyzed cyclization procedure D. The crude material was first dissolved in CH_2Cl_2 , filtered through a plug of silica gel, and concentrated in vacuo. The resultant yellow-brown solid was triturated (10:1 hexanes/ CH_2Cl_2 , 2 \times 5 mL) and filtered to give **3** (33 mg, 49% (procedure C); 14 mg, 21% (procedure D)) as a bright yellow solid: mp 230–250 °C (dec); ^1H NMR (500 MHz, CD_2Cl_2 , 40 °C) δ 7.93 (d, $J = 1.5$ Hz, 2H), 7.92 (d, $J = 1.5$ Hz, 2H), 7.91 (s, 2H), 7.87 (s, 2H), 7.78 (d, $J = 8.0$ Hz, 2H), 7.75 (d, $J = 8.0$ Hz, 2H), 7.69 (dd, $J = 8.0$, 1.5 Hz, 2H), 7.67 (dd, $J = 8.0$, 1.5 Hz, 2H), 7.52 (br s, 4H), 7.46 (d, $J = 1.5$ Hz, 8H), 7.45 (s, 2H), 2.60 (t, $J = 8.0$ Hz, 4H), 1.61 (quint, $J = 8.0$ Hz, 4H), 1.40 (s, 72H), 1.35–1.26 (m, 28H), 0.91 (t, $J = 8.0$ Hz, 6H); ^{13}C NMR (125 MHz, CDCl_3) δ 151.5 (2C), 143.0, 142.8, 138.4, 138.3, 136.4, 136.2, 133.2, 133.0, 132.9, 131.3, 131.1, 127.7 (2C), 127.6, 125.9, 125.8, 125.5, 125.3, 124.8, 124.1, 123.4, 123.3, 122.6, 122.5, 122.3, 121.4 (2C), 83.2, 82.7, 82.6, 81.6, 81.2, 81.1, 81.05, 81.0, 80.9, 80.8, 79.7 (3C), 79.0, 78.7, 78.6, 78.2, 78.1, 35.0 (2C), 32.4,

31.9, 31.5 (2C), 30.3, 29.8, 29.7, 29.6, 29.5, 29.4, 22.7, 14.1; IR (KBr) ν 2952, 2923, 2195, 2133, 1591, 1478, 826 cm^{-1} ; MS (APCI) m/z (%) 2067.5 (M^+ + THF, 40), 1994.7 ($\text{M} + \text{H}^+$, 20), 1935.8 (40), 1617.2 (80), 1507.5 (100); UV (CH_2Cl_2) λ_{max} (log ϵ) 232 (5.24), 324 (5.08), 393 (5.39), 434 (5.24), 453 (5.09).

p-Dibromohexayne. Triyne **10** (612 mg, 1.08 mmol) was reacted with 1,4-dibromo-2,5-diiodobenzene²⁶ (239 mg, 0.490 mmol) at 40 °C using general in situ deprotection/alkynylation procedure B (8 h injection, 8 h additional heating). The crude material was purified by column chromatography (20:1–10:1 hexanes/ CH_2Cl_2) to give the dibromoarene (542 mg, 90%) as a yellow solid: mp 221–226 °C; ^1H NMR (300 MHz, CDCl_3) δ 7.73 (s, 2H), 7.68 (d, $J = 1.5$ Hz, 2H), 7.61 (d, $J = 8.3$ Hz, 2H), 7.51 (dd, $J = 8.3$, 1.5 Hz, 2H), 7.48 (t, $J = 1.5$ Hz, 2H), 7.38 (d, $J = 1.5$ Hz, 4H), 1.39 (s, 36H), 1.20 (s, 42H); ^{13}C NMR (75 MHz, CDCl_3) δ 151.4, 143.6, 138.9, 137.2, 133.2, 131.1, 127.6, 127.3, 126.2, 124.1, 122.6, 122.4, 121.5, 104.5, 96.5, 84.1, 81.9, 78.9, 77.3, 35.0, 31.5, 18.7, 11.3; IR (KBr) ν 2961, 2864, 2210, 2156, 1593, 1467, 1248, 875, 668 cm^{-1} ; MS (APCI) m/z (%) 1293.5 (M^+ + THF, 100), 1222.5 ($\text{M} + \text{H}^+$, 40), 1147.2 (20), 1018.3 (20), 735.5 (40), 447.3 (60).

p-Diiodohexayne 27. A solution of dibromoarene from above (400 mg, 0.320 mmol) in dry THF (30 mL) in a flame-dried flask was cooled to –78 °C under an Ar atmosphere. BuLi (2.5 M in hexane, 0.40 mL, 1.00 mmol) was added and the solution was warmed to –40 °C over 10 min after which I_2 (254 mg, 1.00 mmol) was added. The solution was brought to room temperature, stirred for 15 min, and then quenched with 5% NaHSO_3 (10 mL). The mixture was diluted with Et_2O (30 mL) and washed with 5% NaHSO_3 (2 \times 30 mL) and H_2O (30 mL). The organic phase was dried (MgSO_4) and concentrated in vacuo. The crude material was purified by column chromatography (20:1 hexanes/ CH_2Cl_2) to give **27** (282 mg, 66%) as a yellow solid: mp 132–135 °C; ^1H NMR (300 MHz, CDCl_3) δ 7.94 (s, 2H), 7.70 (d, $J = 1.5$ Hz, 2H), 7.63 (d, $J = 8.3$ Hz, 2H), 7.52 (dd, $J = 8.3$, 1.5 Hz, 2H), 7.49 (t, $J = 1.5$ Hz, 2H), 7.40 (d, $J = 1.5$ Hz, 4H), 1.40 (s, 36H), 1.22 (s, 42H); ^{13}C NMR (75 MHz, CDCl_3) δ 151.4, 143.5, 142.8, 138.9, 133.2, 131.2, 130.6, 127.6, 127.2, 122.7, 122.4, 121.5, 104.6, 98.9, 96.4, 84.2, 81.9, 81.1, 77.5, 35.0, 31.5, 18.8, 11.4; IR (KBr) ν 2958, 2863, 2209, 2154, 1593, 1461, 876, 831, 668 cm^{-1} ; MS (APCI) m/z (%) 1387.2 (M^+ + THF, 20), 1315.3 ($\text{M} + \text{H}^+$, 20), 1291.7 (20), 1261.5 (20), 1177.8 (60), 1102.7 (30), 769.5 (20), 555.2 (100).

Linear Precursor 28. Key piece **8** (400 mg, 0.287 mmol) was reacted with diiodoarene **27** (176 mg, 0.131 mmol) at 55 °C using general in situ deprotection/alkynylation procedure B (22 h injection, no additional heating). The crude material was purified by column chromatography (20:1–10:1 hexanes/ CH_2Cl_2) to give **28** (267 mg, 57%) as an amorphous yellow solid: mp 150–155 °C (dec); ^1H NMR (300 MHz, CDCl_3) δ 7.70 (s, 2H), 7.69 (d, $J = 1.5$ Hz, 2H), 7.672 (d, $J = 1.5$ Hz, 2H), 7.670 (s, 2H), 7.659 (s, 2H), 7.656 (d, $J = 1.5$ Hz, 2H), 7.61 (d, $J = 8.3$ Hz, 4H), 7.60 (d, $J = 8.3$ Hz, 2H), 7.52 (dd, $J = 8.3$, 1.5 Hz, 4H), 7.49 (dd, $J = 8.3$, 1.5 Hz, 2H), 7.47 (t, $J = 1.5$ Hz, 6H), 7.40–7.36 (m, 12H), 1.39 (s, 108H), 1.21 (s, 42H), 1.194 (s, 42H), 1.187 (s, 42H), 1.18 (s, 42H); ^{13}C NMR (75 MHz, CDCl_3) δ 151.4 (3C), 143.5, 143.4, 143.3, 139.0 (2C), 138.9, 137.8, 137.2 (3C), 133.3, 133.2, 133.1, 131.1 (3C), 127.7, 127.6 (3C), 127.4, 127.2 (3C), 125.8, 125.6, 125.3, 124.6, 123.0, 122.8, 122.3 (3C), 121.5 (3C), 104.6 (2C), 104.5, 103.1, 100.2, 96.4 (3C), 84.0, 83.7, 83.3, 81.9, 81.5, 81.3, 80.7 (2C), 80.4, 80.0, 79.4, 79.1, 78.8, 78.0, 77.9, 77.8, 35.0 (3C), 31.5 (3C), 18.7 (4C), 11.4 (3C), 11.3; IR (KBr) ν 2958, 2864, 2203, 2151, 1593, 1474, 668 cm^{-1} ; UV (CH_2Cl_2) λ_{max} (log ϵ) 266 (5.40), 329 (5.28), 351 (5.28), 383 (5.27).

Linear Tetra[18]annulene 4. Acyclic precursor **28** (150 mg, 0.0412 mmol) was subjected to both general Cu-mediated cyclization procedure C and general Pd-catalyzed cyclization procedure D. The crude material was suspended in CH_2Cl_2 (50 mL) and filtered through a plug of silica gel. The annulenic material remained on top of the bed of silica gel was scraped off and transferred to a beaker of refluxing THF (500 mL).

The hot solution was poured through a thin plug of silica gel on a coarse fritted funnel and concentrated in vacuo. The resultant yellow solid was washed with CH_2Cl_2 and filtered to give **4** (28 mg, 26% (procedure C); 10 mg, 9% (procedure D)) as a very insoluble, yellow solid: mp 220–230 °C (dec); solubility too poor for characterization by NMR; IR (KBr) ν 2953, 2903, 2187, 2135, 1591, 1478, 1246, 827 cm^{-1} ; MS (MALDI): m/z (%) 2386.0 ($\text{M}^+ + \text{H}$, 100); UV (CH_2Cl_2) λ_{max} (log ϵ) 274 (5.34), 398(5.59), 462 (5.42).

m-Dibromohexayne. Triyne **10** (800 mg, 1.41 mmol) was reacted with 1,5-dibromo-2,4-diiodobenzene²⁶ (313 mg, 0.641 mmol) at room temperature using general in situ deprotection/alkynylation procedure B (8 h injection, 8 h additional heating). The crude material was purified by column chromatography (20:1 hexanes/ CH_2Cl_2) to give the dibromoarene (700 mg, 89%) as a yellow solid: mp 131.6–133.5 °C; ^1H NMR (300 MHz, CDCl_3) δ 7.89 (s, 1H), 7.69 (d, $J = 1.5$ Hz, 2H), 7.63 (s, 1H), 7.62 (d, $J = 8.3$ Hz, 2H), 7.51 (dd, $J = 8.3, 1.5$ Hz, 2H), 7.48 (t, $J = 1.5$ Hz, 2H), 7.39 (d, $J = 1.5$ Hz, 4H), 1.39 (s, 36H), 1.21 (s, 42H); ^{13}C NMR (75 MHz, CDCl_3) δ 151.4, 143.5, 138.9, 138.4, 136.1, 133.2, 131.1, 127.6, 127.2, 126.7, 124.0, 122.7, 122.4, 121.5, 104.6, 96.3, 83.0, 80.1, 78.7, 77.4, 35.0, 31.5, 18.8, 11.3; IR (KBr) ν 2960, 2864, 2213, 2155, 1593, 1456, 1248, 1060, 876, 830, 677 cm^{-1} ; MS (APCI) m/z (%) 1293.5 ($\text{M}^+ + \text{THF}$, 100), 1222.5 ($\text{M}^+ + \text{H}^+$, 60), 1197.3 (20), 1177.5 (20), 1147.3 (20), 601.3 (20).

m-Diiodohexayne 30. A solution of dibromoarene from above (500 mg, 0.400 mmol) in dry THF (30 mL) in a flame-dried flask was cooled to -78 °C under an Ar atmosphere. BuLi (2.5 M in hexane, 0.50 mL, 1.20 mmol) was added and the solution was warmed to -40 °C over 10 min, after which I_2 (305 mg, 1.20 mmol) was added. The solution was brought to room temperature, stirred for 15 min, and then quenched with 5% NaHSO_3 (10 mL). The mixture was diluted with Et_2O (30 mL) and washed with 5% NaHSO_3 (2 \times 30 mL) and H_2O (30 mL). The organic phase was dried (MgSO_4) and concentrated in vacuo. The crude material was purified by column chromatography (20:1 hexanes/ CH_2Cl_2) to give **30** (335 mg, 62%) as a yellow solid: mp 131.8–134.0 °C; ^1H NMR (300 MHz, CDCl_3) δ 8.41 (s, 1H), 7.71 (d, $J = 1.5$ Hz, 2H), 7.64 (d, $J = 8.3$ Hz, 2H), 7.58 (s, 1H), 7.53 (dd, $J = 8.3, 1.5$ Hz, 2H), 7.50 (t, $J = 1.5$ Hz, 2H), 7.41 (d, $J = 1.5$ Hz, 4H), 1.41 (s, 36H), 1.23 (s, 42H); ^{13}C NMR (75 MHz, CDCl_3) δ 151.4, 147.9, 143.5, 138.9, 137.0, 133.2, 131.2, 129.1, 127.6, 127.2, 122.7, 122.4, 121.5, 104.6, 101.5, 96.3, 83.2, 82.0, 79.5, 77.5, 35.0, 31.5, 18.8, 11.3; IR (KBr) ν 2960, 2863, 2211, 2155, 1593, 1460, 1248, 876, 830, 668 cm^{-1} ; MS (APCI) m/z (%) 1388.2 ($\text{M}^+ + \text{THF}$, 60), 1316.5 ($\text{M}^+ + \text{H}^+$, 90), 1263.5 (50), 1246.5 (60), 1177.8 (100), 767.0 (20), 555.2 (40), 414.2 (90).

Bent Precursor 31. Key piece **8** (400 mg, 0.287 mmol) was reacted with diiodoarene **30** (176 mg, 0.131 mmol) at 55 °C using general in situ deprotection/alkynylation procedure B (22 h injection, no additional heating). The crude material was purified by column chromatography (20:1–10:1 hexanes/ CH_2Cl_2) to give **31** (275 mg, 58%) as an amorphous yellow solid: mp 130–140 °C (dec); ^1H NMR (300 MHz, CDCl_3) δ 7.69 (s, 2H), 7.68 (d, $J = 1.5$ Hz, 2H), 7.663 (d, $J = 1.5$ Hz, 2H), 7.662 (s, 2H), 7.657 (s, 1H), 7.651 (s, 1H), 7.647 (d, $J = 1.5$ Hz, 2H), 7.61 (d, $J = 8.3$ Hz, 4H), 7.60 (d, $J = 8.3$ Hz, 2H), 7.51 (dd, $J = 8.3, 1.5$ Hz, 4H), 7.50 (dd, $J = 8.3, 1.5$ Hz, 2H), 7.46 (t, $J = 1.5$ Hz, 6H), 7.39–7.36 (m, 12H), 1.381 (s, 72H), 1.377 (s, 36H), 1.20 (s, 42H), 1.185 (s, 42H), 1.177 (s, 42H), 1.17 (s, 42H); ^{13}C NMR (75 MHz, CDCl_3) δ 151.4 (3C), 143.5, 143.4, 143.3, 139.0 (2C), 138.6, 137.8, 137.2 (3C), 133.3, 133.2, 133.1, 131.2, 131.1 (3C), 127.8, 127.7 (3C), 127.4, 127.3, 127.2, 127.1, 126.0, 125.8, 125.0, 124.6, 123.0, 122.8, 122.3 (3C), 121.5 (3C), 104.6, 104.5 (2C), 103.1, 100.2, 96.4 (3C), 84.0, 83.7, 83.4, 81.9, 81.6, 81.3, 80.7, 80.6, 80.4, 80.1, 79.4, 79.1, 78.9, 78.1, 78.0, 77.8, 35.0 (3C), 31.5 (3C), 18.8 (3C), 18.7, 11.4 (2C), 11.35, 11.3; IR (KBr) ν 2957, 2864, 2203, 2151, 1593, 1473, 668 cm^{-1} ; UV (CH_2Cl_2): λ_{max} (log ϵ) 265 (5.36), 329 (5.24), 351 (5.22), 400 (5.21).

Bent Tetra[18]annulene 5. Acyclic precursor **31** (150 mg, 0.0412 mmol) was subjected to both general Cu-mediated cyclization procedure C and general Pd-catalyzed cyclization procedure D. The crude material was suspended in CH_2Cl_2 (50 mL) and filtered through a plug of silica gel. The annulenic material remained on top of the bed of silica gel was scraped off and transferred to a beaker of refluxing THF (500 mL). The hot solution was poured through a thin plug of silica gel on a coarse fritted funnel and concentrated in vacuo. The resultant yellow solid was washed with CH_2Cl_2 and filtered to give **5** (1 mg, 1% (procedure C); 33 mg, 32% (procedure D)) as a bright yellow solid: mp 130–140 °C (dec); ^1H NMR (500 MHz, CDCl_3) δ 7.99 (s, 1H), 7.96 (s, 2H), 7.93–7.89 (m, 8H), 7.89 (s, 1H), 7.78 (d, $J = 8.0$ Hz, 2H), 7.75 (d, $J = 8.0$ Hz, 2H), 7.74 (d, $J = 8.0$ Hz, 2H), 7.68–7.62 (m, 6H), 7.50 (br s, 6H), 7.43 (br s, 12H), 1.41 (s, 36H), 1.40 (s, 72H); solubility too poor for ^{13}C NMR; IR (KBr) ν 2963, 2902, 2860, 2762, 2710, 2472, 2451, 2187, 1591, 1476 cm^{-1} ; MS (MALDI): m/z (%) 2385.8 ($\text{M}^+ + \text{H}$, 100); UV (CH_2Cl_2) λ_{max} (log ϵ) 230 (5.29), 395 (5.48), 408 (5.48), 446 (5.38).

Dibromo Star Precursor 33. Key piece **8** (440 mg, 0.316 mmol) was reacted with 1,2-dibromo-4,5-diiodobenzene²⁸ (66 mg, 0.137 mmol) at 45 °C using general in situ deprotection/alkynylation procedure B (24 h injection, 6 h additional heating). The crude material was purified by column chromatography (20:1–15:1 hexanes/ CH_2Cl_2) to give **33** (213 mg, 55%) as an amorphous yellow solid: mp 151–153 °C; ^1H NMR (300 MHz, CDCl_3) δ 7.79 (s, 2H), 7.67 (d, $J = 1.5$ Hz, 2H), 7.66 (s, 2H), 7.65 (d, $J = 1.5$ Hz, 2H), 7.64 (s, 2H), 7.60 (d, $J = 8.3$ Hz, 2H), 7.59 (d, $J = 8.3$ Hz, 2H), 7.48 (dd, $J = 8.3, 1.5$ Hz, 4H), 7.46 (t, $J = 1.5$ Hz, 4H), 7.37 (d, $J = 1.5$ Hz, 8H), 1.38 (s, 36H), 1.37 (s, 36H), 1.18 (s, 42H), 1.17 (s, 42H), 1.16 (s, 42H); ^{13}C NMR (75 MHz, CDCl_3) δ 151.4 (2C), 143.4, 143.3, 139.0 (2C), 137.7, 137.6, 137.3, 137.2, 133.2, 133.1, 131.1 (2C), 127.7, 127.6, 127.4, 127.1 (2C), 125.9, 125.8, 125.1, 124.6, 124.4, 122.9, 122.3 (2C), 121.5 (2C), 104.5 (2C), 103.2, 100.2, 96.4 (2C), 83.7, 83.4, 81.5, 81.3, 80.7, 79.9, 79.7, 79.4, 79.3, 79.0, 78.0, 77.9, 35.0 (2C), 31.5 (2C), 18.7 (2C), 18.6, 11.3 (2C), 11.2; IR (KBr) ν 2956, 2864, 2204, 2148, 1559, 877 cm^{-1} .

Star Precursor 34. Dibromide **33** (200 mg, 0.071 mmol) was reacted with triyne **10** (101 mg, 0.178 mmol) at 60 °C using general in situ deprotection/alkynylation procedure B (8 h injection, 2 h additional heating). The crude material was purified by column chromatography (14:1–9:1 hexanes/ CH_2Cl_2) to give **34** (95 mg, 37%) as an amorphous brown solid: mp 145–150 °C (dec); ^1H NMR (300 MHz, CDCl_3) δ 7.68 (d, $J = 1.5$ Hz, 2H), 7.672 (s, 2H), 7.671 (d, $J = 1.5$ Hz, 2H), 7.664 (s, 2H), 7.661 (d, $J = 1.5$ Hz, 2H), 7.65 (s, 2H), 7.61 (d, $J = 8.3$ Hz, 4H), 7.59 (d, $J = 8.3$ Hz, 2H), 7.50 (dd, $J = 8.3, 1.5$ Hz, 2H), 7.49 (dd, $J = 8.3, 1.5$ Hz, 4H), 7.46 (t, $J = 1.5$ Hz, 6H), 7.38 (d, $J = 1.5$ Hz, 4H), 7.37 (d, $J = 1.5$ Hz, 8H), 1.384 (s, 36H), 1.380 (s, 36H), 1.37 (s, 36H), 1.20 (s, 42H), 1.18 (s, 42H), 1.17 (s, 84H); ^{13}C NMR (75 MHz, CDCl_3) δ 151.5, 151.4 (2C), 143.5, 143.4, 143.3, 139.0 (3C), 137.3 (2C), 137.2, 133.3, 133.2, 133.1, 131.0 (3C), 127.7, 127.6 (2C), 127.4, 127.1 (3C), 125.0, 125.8, 125.1, 124.9, 124.6, 124.5, 123.0, 122.4, 122.3 (3C), 121.5 (3C), 104.5 (3C), 103.2, 100.2, 96.4 (3C), 83.9, 83.7, 83.3, 81.9, 81.5, 81.3, 80.7, 80.6, 80.3, 79.9, 79.1, 78.9, 78.0, 77.9, 77.8, 77.2, 35.0 (3C), 31.5 (3C), 18.7 (3C), 18.6, 11.4 (3C), 11.3; IR (KBr) ν 2954, 2866, 2269, 2203, 2156, 1653, 668 cm^{-1} ; UV (CH_2Cl_2) λ_{max} (log ϵ) 265 (5.42), 328 (5.29), 350 (5.28), 383 (5.27).

Star Tetra[18]annulene 6. Acyclic precursor **34** (90 mg, 0.0247 mmol) was subjected to both general Cu-mediated cyclization procedure C and general Pd-catalyzed cyclization procedure D. The crude material was suspended in hexanes/ CH_2Cl_2 (1:1, 10 mL) and filtered. The crude annulenic material was filtered off and washed with further hexanes/ CH_2Cl_2 (1:1, 10 mL) to give **6** (1 mg, ca. 1% (both procedures)) as a bright yellow solid: IR (KBr) ν 2960, 2921, 2843, 2265, 2192, 1559 cm^{-1} ; MS (MALDI): m/z (%) 2385.1 (M^+ , 100); UV (CH_2Cl_2): λ_{max} (log ϵ) 230 (5.31), 414 (5.42), 428 (5.31), 448 (5.48).

Hexa[18]annulene Precursor 35. Key piece **8** (400 mg, 0.287 mmol) was reacted with 1,2,4,5-tetraiodobenzene (37 mg, 0.064 mmol) at 55 °C using general in situ deprotection/alkynylation procedure B (22 h injection, no additional heating). The crude material was purified by column chromatography (20:1–10:1 hexanes/CH₂Cl₂) to give **35** (139 mg, 42%) as an amorphous brown solid: mp 162–165 °C; ¹H NMR (300 MHz, CDCl₃) δ 7.69 (s, 2H), 7.67 (s, 4H), 7.66 (d, *J* = 1.5 Hz, 8H), 7.65 (s, 4H), 7.60 (d, *J* = 8.3 Hz, 4H), 7.59 (d, *J* = 8.3 Hz, 4H), 7.48 (dd, *J* = 8.3, 1.5 Hz, 8H), 7.46 (t, *J* = 1.5 Hz, 8H), 7.37 (d, *J* = 1.5 Hz, 16H), 1.38 (s, 72H), 1.37 (s, 72H), 1.18 (s, 84H), 1.17 (s, 168H); ¹³C NMR (75 MHz, CDCl₃) δ 151.4 (2C), 143.4, 143.3, 139.0 (2C), 137.3, 137.2 (2C), 133.2, 133.1, 131.0 (2C), 127.7, 127.6, 127.3, 127.1 (2C), 125.9, 125.4, 124.6, 124.4, 122.9, 122.3 (3C), 121.5 (2C), 104.5 (2C), 103.0, 100.3, 96.4, 83.7, 83.3, 81.3, 80.9, 80.7, 80.0, 79.8, 79.4, 79.0, 78.0, 77.9, 77.2, 35.0 (2C), 31.5 (2C), 18.7 (2C), 18.6, 11.3 (2C), 11.2;

IR (KBr) ν 2958, 2864, 2208, 2146, 1473, 668 cm⁻¹; UV (CH₂-Cl₂) λ_{max} (log ϵ) 265 (5.35), 328 (5.24), 349 (5.22), 394 (5.22).

Acknowledgment. This work was supported by the National Science Foundation (CHE-0414175). J.A.M. acknowledges the NSF for an IGERT fellowship. We thank Mojtaba Gholami (University of Alberta) for acquisition of the MALDI data and Annie Tykwinski for her efforts in creating the cover art.

Supporting Information Available: Synthetic details and spectral data for **9**, **12–14**, and **20–22**; copies of ¹H or ¹³C NMR spectra for **3–18**, **20–25**, **27**, **28**, **30**, **31**, and **33–35**. This material is available free of charge via the Internet at <http://pubs.acs.org>.

JO050926V